# The Complex Influences of Back-barrier Deposition, Substrate Slope and Underlying Stratigraphy in Barrier Island Response to Sea-level Rise: Insights from the Virginia Barrier Islands, Mid-Atlantic Bight, U.S.A.

Authors:

Owen T. Brenner
University of Virginia
Department of Environmental Sciences
291 McCormick Road, Clark Hall
Charlottesville, VA 22904-4123
ob9s@virginia.edu
ph: (908) 892-3385
fax: (434) 982-2137

Laura J. Moore
Department of Geological Sciences
University of North Carolina at Chapel Hill
104 South Road, Mitchell Hall
Chapel Hill, NC 27599-3315
laura.moore@unc.edu
ph: (919) 962-5960
fax: (919) 962-4519

A. Brad Murray

Duke University

Division of Earth and Ocean Sciences

Nicholas School of the Environment

Center for Nonlinear and Complex Systems

Duke University

Box 90230

Durham, NC 27708-0230 USA

abmurray@duke.edu

ph: (919) 681-5069

fax: (919) 684-5833

## ABSTRACT

To understand the relative importance of back barrier environment, substrate slope and underlying stratigraphy in determining barrier island response to RSLR (relative sea-level rise), we use a morphological-behavior model (GEOMBEST) to conduct a series of sensitivity experiments, based on late-Holocene hindcast simulations of an island in the U.S. mid-Atlantic Bight (Metompkin Island, VA) having both salt marsh and lagoonal back-barrier environments, and we draw comparisons between these results and future simulations (2000-2100 AD) of island response to RSLR. Sensitivity analyses indicate that, as a whole, the island is highly sensitive to factors that reduce overall sand availability (i.e., high sand-loss rates and substrates containing little sand). Results also indicate that for all predicted future RSLR scenarios tested, islands having high substrate sand proportions (if allowed to migrate freely) will likely remain subaerial for centuries because of sufficient substrate sand supply and elevation to assist in

keeping islands above sea level. Simulation results also lead to basic insights regarding the interactions among substrate slope, back-barrier deposition and island migration rates. In contrast to previous studies, which suggest that changes in substrate slope directly affect the island migration trajectory, we find that—in the presence of back-barrier deposition—the connection between substrate slope and island behavior is modulated (i.e., variability in migration rates is dampened) by changes in back-barrier width. These interactions—which tend to produce changes in shoreface sand content—lead to a negative feedback when the back-barrier deposit contains less sand than the underlying layer, resulting in a stable back-barrier width. Alternatively, a positive feedback arises when the back-barrier deposit contains more sand than the underlying layer, resulting in either back-barrier disappearance or perpetual widening.

**KEYWORDS**

coastal processes, landform evolution, sea-level change, barrier island migration

## 1. INTRODUCTION

### 1.1 Background

Barrier islands comprise over 10% of the world's coastline and are found on every continent except Antarctica (Stutz and Pilkey, 2011). The seaward position, low elevation, and unconsolidated nature of these landforms make them vulnerable to changing conditions, such as rising sea level (e.g., IPCC, 2013), and increasing tropical storm activity (e.g., Knutson et al., 2010). Barrier island response to changing conditions is likely to be complex and variable, and will be determined, in part, by the rate of sand supply (e.g., Wolinsky & Murray, 2009; Moore et al., 2010). Given that most modern barrier islands experience alongshore sand loss, they generally must transgress landward to maintain subaerial exposure as sea level rises (e.g., Curray, 1964; Hayden et al., 1980) and storms become more frequent.

Sand deficiencies initiate island transgression via shoreface erosion and eventual destruction of the primary dune, leading to island narrowing. The resulting island morphology is increasingly susceptible to storm overwash, a process which mobilizes sediment from the shoreface and beach, transporting it landward beyond the dune crest, and depositing it on the back side of the island (e.g., Sallenger, 2000). This cyclical transport regime, also called island rollover, results in a more landward island position through time (e.g., Hayden et al., 1980). If the resulting island position is sufficiently elevated (relative to sea level), the island may begin to stabilize through dune building processes, otherwise, storm overwash and migration will persist. While storm-related overwash events drive island migration over short temporal scales, over long time periods the vertical position of the island relative to sea level dictates the need for landward migration via overwash processes, and therefore RSLR (relative sea-level rise) is the primary influence on long-term island migration.

The response of barrier island systems to RSLR is determined by complex interactions between the geologic framework, physical processes, sediment budget, and human activity (e.g., Cooper, 1994; Pilkey et al., 2000; Gutierrez et al., 2007; Wolinsky & Murray 2009; Moore et al., 2010). For example, the amount of sand in near-surface geologic units influences sand-supply rates (McBride & Moslow, 1991; Moore et al., 2010), while the presence of back-barrier marsh (either salt or freshwater) deposits provides a platform for barrier migration necessitating less landward migration and sediment input to preserve island elevation (e.g., Finkelstein, 1986; Oertel & Woo, 1994; Stolper et.al, 2005). To better understand the likely effect of climate change on barrier islands, it is necessary to assess how different factors (e.g., RSLR rate (RSLRR), sand availability, stratigraphic relationships, variable substrate slopes, etc.) influence island migration. Moore et al. (2010) demonstrate that RSLR rate, followed by sediment supply,

is the most important factor determining barrier island response to climate change for environments in which back-barrier deposition is not a significant factor. They also describe the relationship between island migration trajectory—which is equivalent to average barrier island slope when the sand budget is balanced and equivalent to a less steep "effective" slope when sand-supply is negative—and the slope of the underlying substrate in the absence of a back-barrier unit.

Here, we expand on previous work by providing an assessment of the relative importance of physical characteristics associated with marsh and lagoonal back-barrier environments in determining how barrier islands will likely respond to RSLR. To accomplish this we use the best available geologic observations of an island—the southern half of which is backed by salt-water lagoon and the northern half of which is backed by salt marsh (hereafter referred to as 'lagoon' and 'marsh', respectively)—located on the Eastern Shore of Virginia (Metompkin Island), to develop a suite of late-Holocene (4600 yr bp  present) and future model simulations. Using these simulations we quantify the effect of interactions between the island and back-barrier environments on island response to RSLR by tracking changes in island migration rate and volume. These results allow us to assess the potential range of barrier island response to different future RSLR scenarios as a function of the two different back-barrier environments.

## 1.2 Study Site

The Virginia Barrier Islands (VBIs) are located on the Eastern Shore of Virginia in the mid-Atlantic Bight of the U.S. East Coast (Fig. 1a, b). Twelve of the VBIs, including Metompkin Island, make up The Nature Conservancy's Virginia Coast Reserve (VCR), which has been virtually uninhabited since the 1930's. As one of the most naturally evolving barrier

systems in North America, this area provides an opportunity to study barrier island evolution in the absence of direct human impacts. The VBIs are a mixed energy, tide-dominated barrier island chain (Oertel and Kraft 1994) and as a result the islands are relatively short (in comparison to barrier islands in more wave-dominated regions) and all of the major inlets are stable, having developed in the relict thalwegs of ancient river channels (Halsey, 1979). The northernmost islands of the VCR (Wallops, Assawoman, Metompkin, and Cedar), which exhibit rapid shore-parallel shoreline retreat, form a 40 km concave embayment dominated by erosion (Demarest & Leatherman, 1985) (Fig. 1b). A scarcity of sediment has led to rapid landward migration of these islands and to relatively narrow back-barrier environments, which are connected to the ocean via the permanent tidal inlets between adjacent islands (Rice & Leatherman, 1983). Mechanisms to explain island behavior within this embayment include: limited alongshore sand input from Assateague Island (Rice & Leatherman, 1983); low paleo-topography caused by presence of the ancient Susquehanna or Potomac River valley (Mixon, 1985; Foyle & Oertel, 1997); and a combination of minimal cross-shore input of sand and low topographic relief, due to infilling of paleo-channels with mud (Oertel et al., 2008). The confined lagoonal environments in this area have promoted recent deposition and the accumulation of thick backbarrier deposits, facilitating the establishment of continuous marshes over the past thousand years throughout much of this area (Newman & Munsart, 1968; Van de Plassche, 1990; Oertel & Woo, 1994).

Within the northern section of the VCR, Metompkin Island stretches ~11 km from Gargathy Inlet south to Metompkin Inlet (Fig. 1c). The island has minimal topographic relief (maximum elevation ~3 m) and a relatively constant width of ~200 m. Consistent with the mean VCR migration rate, the island has been transgressing landward ~ 5 m/yr throughout much of the 20$^{th}$ century (Leatherman et al., 1982; Byrnes, 1988). Limited regional sand-supply and rapid

transgression have led to minimal dune development and persistent overwash nearly island-wide (e.g., Wolner et al., 2013). Metompkin Island is divided into northern and southern halves by a mid-island shoreline offset, such that the shoreline of the southern half lies ~200 m west of the northern half (Fig. 1, inset). Following the opening of an ephemeral inlet in 1957 during a storm, the southern half of Metompkin Island migrated at a rate approximately 2.5 times faster than the northern half, resulting in a maximum shoreline offset of 400 m by 1981 (Byrnes, 1988) (Fig. 2). Following inlet closure in 1981, the pattern of dissimilar migration rates reversed and the shoreline has been actively straightening, although an offset still remains. The main effect of this inlet this was to alter alongshore processes and patterns of shoreline change on the ocean side of the island. The major differences in back-barrier environment between the northern and southern halves of the island pre-dated the ephemeral inlet, were not significantly impacted by it, and persisted after its closure. (Note: Given the small size of this inlet relative to the major tidal inlets at the north and south ends of the island, the short period of time during which this inlet was present relative to the lifespan of the barrier island (24 years vs. 4600 years), and our objective to understand the long-term effect of different back-barrier environments on long-term barrier island evolution, we do not explicitly simulate the effects of this ephemeral inlet. However, we do discuss the short-term effects of the opening and closing of this inlet on the alongshore connectivity between the two island halves and therefore on very recent shoreline change rates.)

The northern half of the island is devoid of significant dunes and is backed by a continuous marsh platform, which is exposed in the swash zone providing evidence of active island transgression. The southern half of Metompkin is fronted by discontinuous dunes (max. elevation ~ 3.5 m) interspersed with recent overwash deposits. A fringing marsh (max. width ~50

163 m) is prevalent along the landward margin of the southern half of the island, and is best
164 established in areas of recent overwash, likely due to higher sand input (Fig. 1c).

165 Co-located with the offset on the beach and shoreface, is a transition in the back-barrier
166 environment from platform marsh in the north to shallow open lagoon in the south (Fig. 2). To
167 explain this transition, Byrnes (1988) suggests the importance of underlying pre-Holocene fluvial
168 topography, which slopes downward to the south. More elevated vertical positions along the
169 northern half of the island are thought to have helped marsh vegetation remain subaerial during
170 past RSLR. To the south, sediment deposition (from all sources, including the ephemeral inlet)
171 has not been sufficient to fill the larger void space created by lower initial topography; thus the
172 back-barrier remains inundated and lagoonal conditions persist (Byrnes, 1988).

173 The apparent correlation between differences in back-barrier environment and historic
174 migration behavior (i.e., migration rate, maintenance of island volume, and preservation of
175 general back-barrier/island configuration) on Metompkin make it an ideal location for this study.
176 Additionally, the rapid, shore-parallel migration of Metompkin Island increases the applicability
177 of the 2-D cross-shore model and similar island-wide model constraints for the northern and
178 southern halves of the island (e.g., sand-loss rate, RSLR rate shoreface depth, etc.), allowing us
179 to decipher the influence of differences between the two island halves—primarily in terms of
180 stratigraphy and back-barrier environment—on island response.

181

182 ## 2. SIMULATION DEVELOPMENT

183 ### 2.1 Morphological-behavior modeling with GEOMBEST

184 To simulate barrier island response to RSLR we used the Geomorphic Model of Barrier,
185 Estuarine, and Shoreface Translations (GEOMBEST) (Stolper et al., 2005; Moore et al., 2010;

186 Moore et al., 2014) to develop late-Holocene simulations (hereafter referred to as "base"
187 simulations) for each half of Metompkin Island. Using the base simulations as a starting point,
188 we then conducted sensitivity analyses (varying one parameter at a time) to assess the relative
189 importance of a range of factors in determining barrier island response to RSLR, and future
190 simulations to assess barrier island response to different RSLR scenarios. For all sensitivity
191 analyses and future simulations we determined the average migration rate and final barrier island
192 volume for comparison to base simulation values.

193 GEOMBEST is a two dimensional cross-shore morphological-behavior model that
194 simulates the evolution of island morphology and stratigraphy, including the shoreface, barrier
195 island and back-barrier realms (Fig. 3), in response to RSLR and sand availability across decadal
196 to millennial timescales. Despite seasonal and periodic variations in shoreface morphology
197 (largely associated with storms), shoreface and barrier morphology is generally found to be
198 invariant over long timescales (e.g., Larson, 1991). Thus, we defined (in GEOMBEST) an
199 "equilibrium morphology," which is the shape of the modern surface profile extending from the
200 point where the back-barrier meets the barrier to the base of the shoreface. As sea level rises
201 throughout model simulations, this equilibrium shoreface and barrier profile is shifted landward
202 and upward (representing response to overwash processes) at each time step to the horizontal and
203 vertical position that conserves sand. Throughout model simulations the shape of the barrier and
204 shoreface profile will tend toward the shape of the equilibrium profile, however, maintenance of
205 the equilibrium profile is not prescribed by the model and sufficiently low sand-supply rates,
206 non-erodible substrates, and/or rapid RSLR rates will cause the simulated profile to deviate from
207 the equilibrium profile. What makes GEOMBEST different from similar morphological-
208 behavior models (e.g., Bruun, 1962; Cowell et al., 1995) is that the shoreface and barrier

209 morphology at each time step is influenced by physical characteristics of the underlying
210 stratigraphy. While other models (e.g., Bruun, 1962; Cowell, et al., 1995) assume the sediment
211 below the barrier to be readily available unconsolidated sand, field data (cores, ground
212 penetrating radar) typically indicate compositional heterogeneity. The amount of sand in the
213 substrate (i.e. substrate composition), how easily the substrate can be eroded (i.e., substrate
214 erodibility), and the extent of shoreface exposure of each underlying unit influences how rapidly
215 sand can be liberated from the shoreface. By including these physical constraints, GEOMBEST
216 captures the influence of underlying geology on barrier island migration.

217 ## 2.2 Development of late-Holocene Simulation Inputs

218 To apply GEOMBEST to Metompkin Island, we interpreted findings from the scientific
219 literature to develop a set of plausible initial conditions and to provide estimated values for
220 model inputs (details provided in the subsections that follow). These include geometric
221 constraints necessary to reproduce spatial geologic relationships of the landscape within the
222 model (e.g., stratigraphic relationships), as well as local values for physical processes (RSLR,
223 sand-supply or loss rates, etc.) important to barrier island migration. After developing plausible
224 initial conditions for northern and southern Metompkin Island, we calibrated the model by
225 adjusting model input parameters—within the range of values reported in the scientific
226 literature—to successfully reproduce a back-barrier, barrier, and shoreface morphology similar to
227 the modern configuration over the course of each 4600-year (late-Holocene) base simulation.
228 The resulting final set of input values reflects estimated average rates and parameter values
229 across the late-Holocene period for each island half (as described below and summarized in
230 Table 1). Because the two halves of the island are contiguous, and therefore share similar values
231 for parameters such as alongshore sediment transport rate, shoreface depth, etc., the only

parameters that vary between the northern and southern halves of the island are those describing underlying stratigraphy and back-barrier conditions for which we have geologic and modern evidence to support differences and temporal variability.

### *2.2.1 Initial Morphology and Stratigraphy*

To assist in the development of a plausible set of initial conditions, we developed an average representation of modern morphology (i.e., surface profile, Fig. 4) and underlying stratigraphy for the northern and southern halves of Metompkin Island. To construct a representative surface profile, we combined modern bathymetric data (NOAA National Coastal Elevation Model), LiDAR elevations (NASA: Charts 2005), and mainland Delmarva Peninsula topography (USGS Seamless DEM) extending from the center of the peninsula, across the barrier island system to approximately 45 km offshore. Following methods of Moore et al. (2010), we extended ten shore-perpendicular transects at 1 km increments across the northern and southern halves of the model domain (5 transects on each) and extracted continuous surface elevations along each transect. To create a representative average surface profile for each half of the island, which also serves as the corresponding equilibrium morphology in GEOMBEST, we then calculated an average profile for each group of 5 transects.

Based on interpretations of cores for Metompkin Island and the surrounding area provided by previous investigations (Finkelstein, 1986; Finkelstein & Ferland, 1987; Byrnes, 1988; Wolner et al., 2013), we positioned the top of each identified stratigraphic unit within the upper 20 m at its modern elevation below the surface profile (units include modern barrier island sands, lagoonal deposits and pre-Holocene material). The sand proportion (i.e., percent of the layer that is sand-sized sediment) and erodibility (i.e., an index relating to degree of consolidation) of each unit is specified in the input parameters based on estimates for each unit

from core log data (Table 1). Due to compositional differences, pre-Holocene material is divided into distinct units, with the lowermost unit being a late-Pleistocene fluvial deposit (dark tan unit in Fig. 4) composed primarily of fine to coarse unconsolidated fluvial sand. The upper surface of this unit has been heavily reworked by coastal and fluvial incision and slopes downward, from north to south, in the alongshore direction. Immediately above this layer, is an early-Holocene lagoonal unit (tan unit in Fig. 4) consisting of unconsolidated sandy-silt. Because the elevation of the surface of this unit is influenced by the position of the underlying late-Pleistocene layer, it also dips to the south. In addition to the deeper position of the sandy late-Pleistocene fluvial unit below southern Metompkin Island, due to the presence of different depositional environments, sediment characteristics of the back-barrier unit differ between island halves—the northern back-barrier unit consists of silty marsh material while the southern unit is primarily fine, silty sand (Byrnes, 1988).

Development of initial morphologies and stratigraphies (i.e., the two morphologies and stratigraphies used to represent a plausible starting point for the evolution of each island half in the model) also requires estimation of the cross-shore location of the barrier island at the start of the simulation. Basal peat found 6.6 m below mean sea level (MSL) landward of Metompkin suggests initial submergence of the back-barrier environment during sea level rise 4650 yr bp (Finkelstein, 1986; Finkelstein & Ferland, 1987). Finkelstein and Ferland (1987) use this evidence to suggest the island was located approximately 4km offshore and 6.6 m below the modern position 4650 years ago. This change in elevation over the past 4650 years represents a RSLR rate of 1.44 mm/yr, which is consistent with local historic relative sea-level curves (Newman & Rusnack, 1965; Byrnes, 1988) and regional late-Holocene RSLR rate estimates (Engelhart et al., 2009), further supporting the estimates of Finkelstein and Ferland (1987). In

278 contrast, Byrnes (1988) estimates that approximately 4,600 years ago, when sea level was 6.6 m
279 below its modern position, Metompkin Island was 1.1 km seaward of its current position (though
280 the basis for this estimate was not provided). This estimate appears to be geometrically
281 implausible given geometric constraints imposed by the location of the modern surface profile
282 and published estimates for shoreface depth. Based on the current location of the shoreface (Fig.
283 4), island position 4600 yr bp must have been at least 2 km seaward of the current location, and
284 likely significantly more, assuming any degree of shoreface incision during migration. Based on
285 this analysis, we selected 4600 years ago as the starting point for simulations with the initial
286 barrier island located 4 km offshore and 6.6 m below the modern barrier location. After
287 positioning the barrier island in the model domain, we extended each stratigraphic unit seaward
288 to meet the newly positioned initial surface profiles, resulting in initial island conditions for the
289 late-Holocene simulations of northern and southern Metompkin Island (Fig. 5).

290 ### *2.2.2 Shoreface Depth & Depth Dependent Response Rate (DDRR)*

291 We define the shoreface as extending from the shoreline to the depth beyond which
292 sediment transport is insignificant over long timescales (centurial to millennial). Typically,
293 shoreface depth is deeper than the depth of reworking by fair weather waves and shorter-term
294 engineering definitions for the extent of cross-shore transport (i.e., closure depth), because more
295 extreme (and thus less frequent) storms are more likely to occur as longer timescales are
296 considered (Nicholls et al., 1998). In GEOMBEST, the shoreface depth parameter limits the
297 extent of actively eroding shoreface that can supply sand to a barrier during transgression and it
298 is expressed as the lower limit of the equilibrium morphology and the depth at which shoreface
299 erosion and accretion rates decrease to zero. Following Evert's (1978) method of identifying the
300 long-term limit to significant cross-shore transport as a subtle break in slope, we estimated a

shoreface depth of 6.5 m for Metompkin Island. The maximum potential rate of vertical shoreface erosion (or accretion) as a function of depth (i.e. it is a vertical erosion (or accretion) rate) is defined in GEOMBEST as the Depth Dependent Response Rate (DDRR). This parameter accounts for the decrease in wave orbital velocity with depth, and the corresponding decrease in the ability of wave action to mobilize sediment. Because field studies do not provide guidance on a reasonable estimate for this relationship, similar to previous studies (e.g., Moore et al., 2010), a linear rate of 1 m/yr was extrapolated from sea level (0 m) to a rate of 0 cm/yr at the shoreface depth (6.5 m).

### *2.2.3 Sand-Supply Rate*

GEOMBEST captures the general, time-averaged effects of alongshore sand transport processes via a sand-supply or -loss rate. Because GEOMBEST conserves sand in the cross-shore direction, the sand-supply (or sand-loss) rate reflects the addition or removal of sand (in $m^3/m/yr$) in the alongshore direction. To date there are no published estimates of alongshore transport for Metompkin Island, and for this reason we estimated sand-supply rates based on alongshore sediment transport rates (assuming the majority of sediment transported is sand) for nearby islands (Wallops, Assawoman, and Cedar) (Byrne et. al, 1974; Byrnes, 1988). Given the broad range of values reported (-13.6 to +1.4 $m^3/m/yr$), we relied on the geologic and geometric constraints provided by estimates of past island position, RSLR rate and shoreface depth, adjusting the sand-supply rate last. Successfully reproducing modern conditions in our late-Holocene base simulation for each island half required a sand supply rate of -0.5 $m^3/m/yr$, which falls within the range of reported values. This estimate, which falls at the low end of the range of values estimated for nearby islands, is comparable to the estimated sand-supply rate of -2.3

323 $m^3/m/yr$ derived by Moore et al. (2014) for the Chandeleur Islands from model results of Ellis
324 and Stone (2006).

325 ### *2.2.4 Back-barrier Deposition*

326 To simulate evolution of the back-barrier region during island migration, the vertical
327 position of the back-barrier depositional surface (relative to sea level) is determined by a
328 combination of the back-barrier deposition rate and a maximum back-barrier elevation (formerly
329 referred to in Stolper et al. (2005) as "resuspension depth"). Within GEOMBEST, back-barrier
330 deposition rates (for marshes and lagoons which are connected to the ocean) represent the rate of
331 vertical sediment accumulation upon the uppermost surface of the active back-barrier unit,
332 necessary to maintain elevation relative to sea level. For a particular back-barrier morphology to
333 persist (both in the vertical and horizontal dimensions) over long periods of time, this rate of
334 deposition must be comparable to the RSLR rate. When back-barrier sediment accumulates
335 slowly, more sand, transported via overwash processes, will be needed to fill the area behind the
336 barrier (sometimes referred to as back-barrier accommodation space) to maintain island elevation
337 relative to sea level as sea level rises. When back-barrier sedimentation is rapid, the back-barrier
338 may fill in, allowing conversion of lagoon to marsh, for example. Acting to oppose such effects
339 of rapid back-barrier deposition within the model, the elevation of the back-barrier region
340 (relative to sea level) is limited by a maximum back-barrier elevation. In reproducing the
341 present-day thickness of marsh and lagoonal sediments GEOMBEST implicitly accounts for the
342 effects of compaction of back-barrier sediments, which given thicknesses of only 1-1.5 m in our
343 study area, should be minimal.

344 While back-barrier environments are variable throughout the VCR, the general
345 distribution of marsh platform (northern half of the island) and open lagoon (southern half of the

346 island) has remained unchanged since the earliest recorded surveys (1852), suggesting that the
347 rate of infilling of the back-barrier environments has kept up with RSLR. Additionally, over
348 long timescales, vertical deposition rates of both subaerial marsh platforms (Van de Plassche,
349 1990; Oertel & Woo, 1994) and shallow open bays (Nichols, 1989) have been found generally to
350 mirror the rate of RSLR. Therefore, during late-Holocene simulations, we set the infilling rates
351 of both marsh and open lagoon equal to the historic RSLR rate of 1.44 mm/yr (see section 2.2.1
352 for derivation of this rate). A maximum back-barrier elevation of -0.4 m (average water depth of
353 modern lagoon) for southern Metompkin Island maintains lagoon depth through time to avoid
354 back-barrier infilling, and a value of +0.14 m (modern average marsh elevation) for northern
355 Metompkin Island limits vertical marsh accretion to within +0.14 m of sea level at any given
356 time. In this way, and as suggested by observations over the last 1.5 centuries, we do not allow
357 marsh conversion to open water or vice-versa.
358

359 ## 3. EXPERIMENTS, RESULTS AND INTERPRETATIONS

360 The two calibrated late-Holocene simulations (arising from the development of initial
361 conditions and input parameters described in the previous section) (Fig. 6) closely reproduce the
362 modern configuration with the offset between the final simulated time step (representing
363 calendar year 1950) and the actual modern surface (calendar year 2005) being as expected given
364 the time difference between the two (Fig. 7). Average island migration rate (m/yr) is equal to the
365 slope of the linear regression of shoreline position through time. Barrier island volume, reported
366 in $m^3/m$, represents island volume at the final simulated time step and is calculated by integrating
367 to find the cross-shore area above the substrate surface and under the portion of the surface
368 profile representing the barrier island. In addition to migration rate and final island volume—to

allow more detailed descriptions and comparisons of island and back-barrier evolution—we also made supplementary measurements (e.g., back-barrier width, barrier island slope, and substrate slope) for select simulations. As a reference point for comparison with sensitivity experiments and future simulations, average island migration rate was slightly slower in the base simulation for northern Metompkin Island (0.76 m/yr) than it was in the base simulation for the southern half of the island (0.78 m/yr), whereas final barrier island volume was slightly larger (1280 $m^3$/m/yr vs. 1000 $m^3$/m/yr for the north and south, respectively).

As in Moore et al. (2010), we define average barrier island slope as the slope of a line extending from the base of the shoreface to the point where the island meets the back-barrier (Fig. 3). Here, base simulation values for sand-loss rate are only slightly negative (-0.5 $m^3$/m/yr) and therefore average barrier island slope closely approximates effective barrier island slope (the slope adjusted for sand loss)—for this reason we refer only to average barrier island slope when using this quantity to make comparisons. Additionally, because over long timescales back-barrier deposition occurs increasingly landward on top of the underlying substrate as the island migrates, we use the term substrate slope to characterize the slope of the surface of the uppermost stratigraphic unit immediately behind (and underneath) the back-barrier, rather than the slope of the back-barrier depositional surface (Fig. 3).

### 3.1 Sensitivity Analyses

We systematically adjusted back-barrier sedimentation rate, sand-supply rate, substrate composition, substrate erodibility, DDRR, shoreface depth and RSLR rate for independent simulations of north and south Metompkin within the range of values indicated in Table 1. To extend the applicability of these results to other similar coastal environments we varied input parameters not only within, but also just beyond, the range of published values for the VBIs. To

test the sensitivity of the overall barrier system and identify possible thresholds that might induce changes in island state we also varied some parameters (e.g., RSLR rate) beyond expected natural variation.

### *3.1.1 Back-barrier Sedimentation Rate*

When rates of back-barrier sedimentation are low relative to the sea-level rise rate (0.5 mm/yr), a continuous back-barrier deposit (i.e., marsh and lagoonal) does not form, likely because the RSLR rate (1.44 mm/yr) outpaces deposition. In the absence of persistent back-barrier deposits, island volume is larger and migration rates are high (Figs. 8a, 9a) as the island moves farther inland and gains volume to maintain vertical elevation above sea level without the assistance of an underlying back-barrier unit. This is especially true for southern Metompkin Island where lower substrate slopes and a lower elevation of the underlying sand-rich stratigraphic unit, relative to the northern half of the island, enhances landward migration in response to given RSLR. When back-barrier sedimentation rates approach or slightly exceed RSLR rate (1 – 1.5 mm/yr), marsh (north) and lagoonal (south) units become well-developed by the final time step and final island volume decreases (Fig. 9a) as back-barrier deposits, instead of island sand, fill the accommodation space behind the barrier, thereby requiring less removal of sand from the shoreface and less landward migration to achieve a vertical elevation above sea level. When sedimentation rates exceed RSLR rate (>1.5 mm/yr), vertical accumulation of back-barrier deposits is limited by the resuspension depth, and the horizontal extent of the back-barrier remains unchanged.

### *3.1.2 Sand-Supply Rate*

As the rate of sand supply increases (from sand removal to addition of sand) final barrier island volume increases rapidly and migration rates decline (Figs. 8b, 9b). An increase in sand-

supply rate of 2 $m^3$/m/yr (from -1 to 1 $m^3$/m/yr) results in a ~100% increase in final island volume for both northern and southern Metompkin Island. While changes in overall barrier volume are nearly identical between the north and south, varying the sand-supply rate results in a greater disparity in migration rate change. Southern Metompkin Island migrates more rapidly at lower sand-supply rates than northern Metompkin Island, suggesting that migration of the southern half is relatively more sensitive to equal decreases in barrier island volume generated by lower sand-supply rates than northern Metompkin Island. This may be explained by the lower substrate surface beneath south Metompkin, which likely requires island volume to play a larger role in maintaining vertical position.

#### *3.1.3 Substrate Sand Percentage*

By assessing barrier island sensitivity to changes in the percentage of sand contained in each stratigraphic unit, we seek to determine the relative importance of individual units in supplying sand to the island. The effect of an individual stratigraphic unit on average migration rate and final barrier island volume is largely determined by the proportion of the shoreface the unit is exposed along, and how that proportion changes throughout a simulation. Differences in underlying stratigraphy and topography between island halves account for different amounts of exposure of each stratigraphic unit along the shoreface. For this reason, the relative influence of each stratigraphic unit on island behavior varies slightly between the north and south (Fig. 10). Island behavior is most sensitive to changes in the percentage of sand in the barrier island, likely because this parameter affects both the sand-supply rate (as the barrier is eroded) and the amount of sand that is needed to maintain the island above sea level. Beyond this, island behavior appears to be slightly more sensitive to changes in the sand percentage of the early-Holocene lagoonal unit in the north and the back-barrier marsh unit (although only marginally) in the

438 south—likely because these are the most prevalent units exposed along the shoreface throughout
439 the late-Holocene simulation.

440 ### 3.1.4 *Substrate Erodibility*

441 Consistent with Moore et al. (2010), island response to RSLR is relatively insensitive to
442 substrate erodibility (Fig. 11). Sensitivity analyses indicate that island volume and migration
443 rate are only affected when underlying stratigraphic units are 1000 times less erodible (i.e.,
444 erodibility index = 0.001) than instantaneously erodible unconsolidated sediments (i.e.,
445 erodibility index = 1). However, given the loosely consolidated silty muds and fine sands
446 beneath the VBIs (as opposed to lithified rock which might better represent erodibility values of
447 0.001) it is unlikely that the stratigraphic units here can resist erosion to a degree that would
448 significantly impact large-scale island behavior.

449 ### *3.1.5 Depth-Dependent Response Rate*

450 Also consistent with the results of Moore et al. (2010), barrier island evolution appears to
451 respond differently to changes in vertical erosion rates than it responds to changes in the other
452 parameters. As DDRR decreases, final island volume and migration rate are unchanged for both
453 island halves for all values of DDRR above 2 cm/yr. At (very low) values of less than 2 cm/yr
454 sharp increases in average migration rate and decreases in final island volume occur with
455 decreasing DDRR (Figs. 8c, 9c). This suggests there is a threshold shoreface erosion rate below
456 which barrier island evolution responds dramatically. For example, if shoreface erosion rates
457 begin to limit the degree to which the shoreface evolves, shoreface shape must change over time
458 (e.g., shoreface depth would decrease and the assumption of an equilibrium shoreface would no
459 longer apply) and new island behaviors would emerge (e.g., detachment from lower shoreface,
460 drowning, etc.).

### *3.1.6 Shoreface Depth*

Greater shoreface depths (4−9 m) result in a trend of increasing island volume and decreasing migration rate, because deeper shoreface depths allow extraction of sand from a greater proportion of the bathymetric profile (Figs. 8d, 9d) and therefore yield more sand per meter of landward migration. The differences in island behavior between northern and southern Metompkin Island throughout this range of shoreface depth values is most likely due to differences in underlying stratigraphy (i.e., a more vertically elevated sand-rich late-Pleistocene fluvial deposit in the north) which allow the northern half to liberate more sand per increment of landward migration, particularly at shoreface depths >7.5 m. Similar to the results of the sand-supply sensitivity experiments (section 3.1.2), although shallow shoreface depths (<6 m) result in similar patterns of island volume decrease for both island halves, the migration rate of southern Metompkin appears to be more highly sensitive to this reduction in sand availability associated with a shorter active shoreface than the migration rate of northern Metompkin. Although barrier island behavior appears sensitive to shoreface depths ranging from 4–9 m, when considering only response to the range of depths reported in the literature (5.5–8 m) volume and migration rate are fairly insensitive to changes in shoreface depth.

### *3.1.7 Relative Sea-Level Rise Rate (RSLR rate)*

To assess the sensitivity of island behavior to RSLR rate, we increase the RSLR rate from 0.5 mm/yr to 4 mm/yr in 0.5 mm/yr increments while keeping the total amount of RSLR constant at 6.5 m of total change across all simulations (constant total sea level simulations). Unlike simulations in which the duration of the simulation was held constant (i.e., the constant duration RSLR rate simulations discussed below), in the constant total RSLR simulations the island traverses an identical substrate (slope and composition) throughout each model run, thereby

484 eliminating the effects of variable substrate slopes on simulation results. This requires each
485 simulation to run for a different length of time ranging from 1,600 years for the 4 mm/yr
486 simulation to 13,200 years for the 0.5 mm/yr simulation.

487 Considering the constant total RSLR experiments, landward migration is faster at higher
488 RSLR rates (Figs. 8e, 9e) as expected. Interestingly and unexpectedly, at RSLR rates (and
489 therefore back-barrier sedimentation rates) ≤1 mm/yr, back-barrier environments struggle to
490 persist throughout simulations of both northern and southern Metompkin Island. At low sea-
491 level rise rates northern Metompkin Island adjusts to changing conditions primarily through
492 increases in island volume, whereas southern Metompkin Island adjusts through increases in
493 landward migration rates (Figs. 8e, 9e). As in the sensitivity to changes in shoreface depth, this
494 difference in island behavior is likely explained by the lower position of the sand-rich
495 Pleistocene unit in the south, which requires higher rates of landward migration to extract the
496 same amount of sand per unit of RSLR as in the north (Fig. 5).

497 When RSLR rates are faster than 1 mm/yr, migration rates increase linearly for both
498 island halves, final island volume changes little (Figs. 8e, 9e), and island morphology (i.e., island
499 shape, back-barrier width) remains unaffected. This suggests that final back-barrier, island, and
500 shoreface morphology are minimally affected by changes in island migration rate alone—which
501 is more directly controlled by RSLR rate—when the length, composition, and slope of the
502 underlying substrate surface the island traverses are held constant.

503 In the second set of RSLR rate sensitivity experiments we, again, increase RSLR rates
504 from 0.5 to 4 mm/yr in 0.5 mm/yr increments, but to assess the impact of substrate slope
505 variability on final island configuration, all simulations have a constant duration of 4600 years
506 (Figs. 8f, 9f). This requires the barrier to migrate progressively farther landward across

mainland terrain of varying slope as RSLR rates increase. According to Moore et al. (2010) (who did not consider the effects of a co-evolving back-barrier unit) island volume should adjust until the barrier island slope (or "effective" barrier island slope in the case of a non-zero sand-supply rate or a substrate that is less than 100% sand) approaches equilibrium with substrate slope. Our incorporation of a simultaneously evolving back-barrier unit, however, may limit the direct applicability of these general relationships, requiring additional examination of substrate slope as well as island, and back-barrier behavior at different RSLR rates.

Considering the constant duration experiments, for RSLR rates between 0.5 and 1.0 mm/yr, final barrier island volume increases with increasing RSLR rates for both northern and southern Metompkin Island but the increase is greater in the north than in the south (67% vs. 18% when comparing final barrier island volume for RSLR rate= 0.5 and RSLR rate= 1 mm/yr) (Fig. 9f). This is likely due to a greater cumulative substrate sand percentage along the shoreface in the north, which generates more sand per increment of landward migration than in the south. At higher RSLR rates of 1–4 mm/yr, island response reverses such that final barrier island volume in the north decreases by 46% whereas final barrier island volume increases 66% in the south. Across this RSLR rate interval, migration rates increase with increasing RSLR rates but the rate of increase is slower for southern Metompkin (by 5-13%) than for northern Metompkin—at RSLR rate of 4 mm/yr northern Metompkin migrates a total of 0.9 km farther than southern Metompkin (Fig. 8f). These differences in final barrier island volume and migration rate likely occur because, at higher RSLR rates, and therefore longer migration pathways, the composition of the back-barrier unit (15% sand in the north vs. 60% in the south) strongly influences the average sand content of the substrate exposed along the length of the shoreface (hereafter referred to as the shoreface-substrate sand content). The sand-poor back-

barrier unit in the north results in a lower shoreface-substrate sand content, which leads to a smaller, more rapidly migrating island. In comparison, the relatively sand-rich back-barrier unit in the south results in a relatively higher shoreface-substrate sand content, which leads to a relatively larger island that migrates landward less rapidly. This finding suggests that the island halves adjust toward equilibrium in different ways because of their stratigraphic differences.

Comparisons of final back-barrier width, substrate slope and island volume further illuminate the relationships described above. A comparison of final back-barrier width and the slope of the additional length of substrate traversed as compared to that of the next lowest RSLR rate simulation (i.e., additional-substrate-length slope), indicates that the horizontal width of the back-barrier region (in both the north and south) tends to increase when the island is migrating across a gently sloping substrate (i.e., slopes near or below 1 m/km) (Fig. 12a). For example, the additional-substrate-length slopes encountered by southern Metompkin Island are more consistently gentle (<1 m/km) across most RSLR rate simulations (Fig. 12a light gray lines; e.g., Fig. 13b) leading to widening of the back-barrier across most simulations. In contrast, for simulations having a higher cumulative RSLR (e.g., above 1.5 mm/yr), northern Metompkin Island migrates over a steep substrate allowing for only brief periods of rapid widening of the backbarrier (Fig. 12a dark gray lines; e.g., Fig. 13a). In these experiments, then, migration across steep substrates tends to cause back-barrier width to remain constant (e.g., both islands) or to decrease (e.g., northern Metompkin Island only) and low substrate slopes (congruent with back-barrier widening, and consistent with results from Stolper et al. (2005)) allow for the deposition of a more expansive back-barrier unit providing a thicker back-barrier deposit upon which future island migration will occur (Fig. 13). The decrease in island volume for northern Metompkin Island and increase in island volume for southern Metompkin as RSLR rates

553 increase from 1 mm/yr to 2.25 mm/yr (Fig. 12b) discussed above, corresponds with periods of
554 back-barrier widening (associated with low substrate slope) on both island halves. Because
555 widening of the back-barrier results in a thicker back-barrier unit, this increases the proportion of
556 the shoreface along which back-barrier deposits are exposed. This, in turn, increases the
557 importance of the back-barrier unit in determining the shoreface-substrate sand content. In the
558 north a thicker back-barrier deposit results in a decrease in shoreface-substrate sand content
559 (because the back-barrier is only 15% sand) and therefore a shallower effective barrier island
560 slope/migration trajectory (i.e., faster migration rates) leading to a decrease in island volume
561 (Table 3). In contrast, thickening of the back-barrier deposit in the south leads to an increase in
562 the shoreface-substrate sand content (because the back-barrier is 60% sand) and therefore a
563 steeper effective barrier island slope/migration trajectory (i.e., slower migration rates) and an
564 increase in island volume (Table 3).

565 ### 3.2 Future Simulations

566 To explore the range of potential future barrier island response to RSLR, we conducted a
567 suite of simulations extending from 2000 AD to 2100 AD in 5-year time steps (e.g., Fig. 14).
568 While these future simulations are based on the same values derived from the calibration of the
569 late-Holocene simulations (Table 1), and incorporate well-supported estimates for future RSLR
570 rates, they are not intended to be accurate representations of future island evolution, but rather to
571 capture a wide range of possible future island response, and to facilitate further exploration of
572 interactions among increased RSLR rates, substrate slope and variations in stratigraphy. Unlike
573 the late-Holocene simulations, in future simulations, northern and southern Metompkin Island
574 migrate across known topographic surfaces which are more variable in slope (Fig. 14) than the
575 conceptualized initial condition for the late-Holocene simulations (Fig. 4).

576 Reported values for eustatic RSLR by the year 2100 AD range from 0.26 m to 1.6 m,
577 (Grinsted et al., 2009; Jevrejeva et al., 2010; IPCC 2013). Because local RSLR rates are
578 expected to be slightly faster than eustatic rates we chose to vary RSLR between 0.6 and 1.6 m
579 of total rise over 100 years. Given uncertainties regarding the total amount of RSLR by 2100
580 and the nature of RSLR acceleration, we simulated multiple RSLR scenarios, including a
581 constant RSLR rate, a linearly increasing RSLR rate, and a RSLR rate that increases along a
582 polynomial curve. In these simulations, we allow back-barrier sedimentation rates to keep pace
583 with increases in RSLR.

584 Studies have shown that vertical accumulation rates within the back-barrier, (including
585 both marsh and lagoonal environments), have a finite upper limit considerably below some
586 future RSLR rate predictions thereby resulting in the likely submergence or deepening of back-
587 barrier environments in the future (e.g., Craft et al., 2009; Kirwan et al., 2010). To explore how
588 a back-barrier sedimentation rate that is lower than the RSLR rate may influence island
589 migration we performed additional simulations in which back-barrier sedimentation rate is
590 limited to 10 mm/yr. This estimated rate is derived from model simulations of vertical marsh
591 accumulation during accelerated RSLR by Kirwan et al. (2010), and is meant to represent a
592 conservative upper limit to rates of back-barrier sedimentation. We use this estimate in
593 simulations of both island halves, given the lack of analogous estimates for back-barrier
594 sedimentation in lagoonal environments where riverine sediment influx is minimal. To explore
595 the effects of a possible lag between accelerations in RSLR and corresponding changes in back-
596 barrier sedimentation rate, as reported by Kirwan and Temmerman (2009), we also conducted a
597 series of simulations in which back-barrier sedimentation rates are limited to 10 mm/yr with
598 increases in sedimentation rates being offset from RSLR rate by 20 years.

599 Island migration rate and final island volume remain fairly constant for a given amount of
600 cumulative RSLR regardless of whether the rate of increase is constant or follows a linear or
601 polynomial curve (Fig. 15). This implies that the rate at which the RSLR rate increases over
602 time has less of an impact on migration rates than the cumulative amount of RSLR, and
603 variations in substrate slope or composition. Substrate slope and composition are relatively
604 constant between 2000-2100 AD for all RSLR scenarios (0.6-1.6 m), but differ between northern
605 and southern Metompkin Island (see Modern Configuration, Fig. 4). During the 100-year-long
606 future simulations, northern Metompkin Island migrates faster and gains more volume than
607 southern Metompkin Island, regardless of the RSLR scenario (Table 2 & Fig. 15). Island
608 migration rates during the first 20 years of the future simulations (7 to 8.6 m/yr in the north
609 versus 4.5 to 6 m/yr in the south for a range of cumulative RSLR values) are in general
610 agreement with average observed shoreline change rates for 1985 – 2009 (7 m/yr in the north vs.
611 ~2 m/yr in the south calculated from shoreline position data from Wolner (2011)).
612 Consistent with the back-barrier sedimentation rate sensitivity experiments presented in
613 section 3.1.1, when the back-barrier sedimentation rate is less than the RSLR rate (e.g., future
614 simulations in which back-barrier sedimentation rate is limited to 10 mm/yr, both with and
615 without a 20 year lag) final island volume changes similarly for both island halves (Fig. 15b). In
616 contrast, the migration rate of southern Metompkin Island is more sensitive to limited back-
617 barrier sedimentation rates than northern Metompkin Island, particularly when RSLR is high
618 (Fig. 15a). Differences between the behavior of northern and southern Metompkin are likely the
619 result of differences in landward substrate slope and substrate sand content. At the start of future
620 simulations northern Metompkin Island is positioned atop a backbarrier unit containing limited
621 sand (15%) and is backed by both subaerial marsh and steeply inclined mainland topography,

622 whereas the back-barrier unit behind and below southern Metompkin Island contains more sand
623 (60%) and has a more gently sloping mainland topographic surface along its landward edge (Fig.
624 4, modern configuration is the initial condition). The slope of the landward substrate appears to
625 influence the ability of the back-barrier to maintain its initial width during RSLR. In a fashion
626 similar to the relationship described at the end of section 3.1.7, steeper substrate slopes (i.e.,
627 behind northern Metompkin Island) do not allow for back-barrier widening, and may even
628 reduce back-barrier width, but when landward substrate slope is gentler (<1 m/km as in the case
629 of southern Metompkin Island) the area over which back-barrier deposition takes place increases
630 resulting in a thicker back-barrier deposit.

631 Limitations to back-barrier sedimentation rate appear to amplify the effect of steep
632 substrate slopes on back-barrier width. During future simulations when back-barrier
633 sedimentation rate equals RSLR rate, the substrate slope landward of southern Metompkin Island
634 is never sufficiently steep to cause back-barrier narrowing, regardless of the amount of
635 cumulative RSLR by 2100 (e.g., Fig. 14). However when simulating the same RSLR rate
636 scenario with a limited back-barrier sedimentation rate, back-barrier width is constricted
637 resulting in a thinner back-barrier deposit and thus a lower shoreface-substrate sand content,
638 which decreases the effective barrier island slope leading to faster landward migration (e.g., at
639 cumulative RSLR $\geq$ 1 m on southern Metompkin Island) (Fig. 15a, dashed green, aqua and
640 orange lines vs. other dashed lines), suggesting that limitations on back-barrier deposition have
641 the potential to strongly influence future island behavior.

642 To briefly explore how an island like Metompkin might respond to conditions more
643 extreme than suggested by current RSLR predictions, we ran additional simulations using
644 combinations of more extreme rates of RSLR rate and sand loss. Independently, we simulated

island response to 2–5 m total RSLR (at intervals of 0.5 m) by the year 2100 and sand-loss rates ranging from 0.5–35 $m^3$/m/yr (in progressively larger intervals). Both sets of simulations include RSLR rates that increase polynomially and back-barrier sedimentation rate limits of 10 mm/yr to aid in simulation of most extreme conditions. Across all extreme RSLR rate simulations, increases in RSLR rates result in accelerated migration rates (ranging from 10 m/yr to 33 m/yr) for both halves of Metompkin Island, and never does the island appear unable to keep pace with RSLR. In simulations of northern and southern Metompkin Island, migration rates increase linearly as sand-loss rates increase, and, as in the future simulations involving more realistic representations of future conditions, northern Metompkin Island migrates considerably more rapidly than its southern counterpart. These simulations suggest that if migration can occur freely in the future, barriers having characteristics similar to Metompkin Island may respond, even to extreme conditions, via increases in migration rates rather than by disintegration and submergence. These results also suggest that barrier island overstepping is not likely to occur unless an island is too wide or the associated shoreface erodes too slowly for the system to migrate via rollover (e.g., Mellett et al., 2012), or unless other factors such as very rapid sea-level rise and/or cementation (e.g., Green et al., 2014) are at work.

# 4. DISCUSSION

## 4.1 Model Limitations

When simulating past and future island migration during RSLR, it is important to consider model limitations and assumptions when interpreting model results. The morphological-behavior approach illuminates important mechanisms of island migration within the given study site and beyond, but generally restricts interpretations to theoretical and qualitative assessments of the range of potential island behavior. For example, here, we condense the long-term

668 migration of an 11 km long barrier island to two (i.e., north and south), 2-D cross-shore domains
669 and conduct a suite of simulations each having a handful of input parameters such that the
670 resulting island behaviors represent the potential average response to RSLR for that island
671 segment. We also purposely treat each island half as an independent island (without considering
672 how alongshore processes redistribute sand and realign the beachface and shoreface between
673 island halves) so that we may explore the role of variations in back-barrier environment and
674 underlying stratigraphy within a single island thereby reducing the number of dissimilar
675 characteristics influencing island response. Future island response to RSLR on Metompkin
676 Island itself is more likely to fall somewhere between the simulated behaviors of the two island
677 halves. Some short-term island behaviors (e.g., opening and closing of ephemeral inlets and
678 development of shoreline offsets) are not included in these model simulations, but could play a
679 role in past and future island behavior within any barrier island system, and may be critically
680 important in more wave-dominated settings. Additionally, GEOMBEST does not simulate
681 changes in island behavior due to variations in storm activity. Future deviations from time-
682 averaged storm activity in the past (e.g., Knutson et al., 2010) may alter future island response
683 beyond the range of potential behavior simulated here. For all of the reasons outlined above, we
684 do not intend for our simulations to accurately portray island response at any one location along
685 Metompkin Island, or to be predictive in a quantitative way, but rather to yield insights into the
686 factors most important in controlling barrier island behavior in general.

687 Across all simulations of Metompkin Island, the accumulation of back-barrier deposits
688 through time assumes a constant input of sediment to the back-barrier environment without
689 accounting for where this sediment is derived from. In reality, much of the sand deposited in the
690 back-barrier originates from the nearshore zone and is transported landward by overwash

691 (particularly for southern Metompkin Island) and/or inlet processes and thus, back-barrier
692 sedimentation is actually closely linked with alongshore sand supply. By simulating island
693 response under the assumption that back-barrier sedimentation is independent from sand supply
694 processes, we have not accounted for potential reductions in sand availability to the island that
695 may result from the transfer of overwash sand to the back-barrier. Future work exploring and
696 simulating explicit coupling of sand supply rates and back-barrier sedimentation rates within
697 GEOMEBST will be useful and allow more accurate depictions of the interactions between the
698 nearshore and back-barrier environments (e.g., Walters et al., 2014). Coupling future iterations
699 of GEOMBEST with models that more explicitly treat alongshore variability and inlet dynamics
700 (e.g., McNamara and Werner, 2008), would assist in providing additional insights for wave-
701 dominated barrier islands.

702 ### 4.2 Insights on Local Geologic Constraints

703 Interestingly, through development of an initial late-Holocene morphology and
704 stratigraphy for northern and southern Metompkin Island and pairing of these configurations
705 with estimated values from the literature for shoreface depth and historic island position it
706 becomes evident that some published estimates of mid-Holocene island position are
707 geometrically implausible. Based on the constraints listed above we find that island position
708 4600 yr bp must have been at least 2 km seaward of the current location, and likely was
709 significantly more, assuming any degree of shoreface incision during migration. Just as
710 preparations for conducting simulations sheds light on island position ~4600 years ago, the
711 simulations themselves are consistent with and appear to corroborate published estimates for the
712 timing of establishment of back-barrier deposition. For the first ~3500yrs of the late-Holocene
713 base simulations both halves of Metompkin Island migrate landward with little to no

accumulation of back-barrier sediment. Once the island reaches a stretch of more gently sloping substrate (near 40000 km on the x-axis in Fig. 13) a continuous back-barrier unit begins to form. The timing of initial back-barrier deposition, predicted by the simulations, matches well with reported ages for the formation of the modern lagoon and marsh system (Van de Plassche, 1990).

### 4.3 Sand Availability

Because underlying stratigraphic units exposed along the shoreface are critical in supplying an island with sand, differences in substrate sand content have a significant impact on island behavior (i.e., island migration rates and island volume). The sand content of material exposed along the shoreface differs between northern and southern Metompkin Island due to differences in underlying stratigraphy (primarily related to the relative position of the late-Pleistocene fluvial deposit) and the sand content of back-barrier deposits. The sand content of backbarrier deposits will tend to be different for open versus closed back-barrier environments because open back-barrier environments will tend to receive sand from shorelines via tidal currents, resulting in sandier back-barrier deposits. In comparison, barrier systems having closed (and therefore brackish or fresh-water back-barrier environments) will tend to produce back-barrier deposits that are relatively lower in sand content because they do not receive sand via tidal currents. Although both the lagoon and marsh environments in our study site are connected to the open ocean shoreline via nearby permanent inlets, insights into the dependence of barrier and backbarrier evolution on sand content are generally applicable to barrier systems associated with either open or closed back-barrier environments.

In addition to fluctuations in back-barrier sand content, the shoreface-substrate sand content also fluctuates throughout the simulations as the island traverses across different stratigraphic units (Fig. 16). Both portions of the island experience a decline in shoreface-

737 substrate sand content during the first ~2300 years as the shoreface progresses into a more sand
738 deficient unit (early-Holocene lagoonal deposit). However, this decline is slightly less on
739 northern Metompkin Island due to the higher vertical position of sand-rich units (late-Pleistocene
740 fluvial deposit) (Fig. 4). During the second 2300 years of the modeled time period, back-barrier
741 deposits begin to compose the bulk of the shoreface allowing differences in back-barrier sand
742 content to further perpetuate a decline in northern shoreface-substrate sand content and a slight
743 increase in the southern shoreface-substrate sand content. This difference in back-barrier sand
744 content leads to the greatest disparity in island response when simulating barrier island migration
745 significantly landward of current island position (i.e., RSLR rate sensitivity analyses having
746 constant duration and simulations of future barrier island response).

747 Although the main differences between island response in the north and south result from
748 differences in shoreface-substrate sand content, the island as a whole is also highly sensitive to
749 changes in sand-supply rate. If the two island halves become disconnected (as they were when
750 an inlet separated them), the south will tend to migrate more rapidly than the north because the
751 shoreface-substrate sand content is lower. Such an inherent difference may have led to
752 development of the modern shoreline offset. However, when the two island halves are connected
753 via alongshore transport (as they have been since the inlet closed), the tendency for gradients in
754 alongshore transport to smooth out the shoreline will ultimately equalize northern and southern
755 migration rates. This case study, therefore, suggests that although differences in shoreface-
756 substrate sand content will tend to lead to differences in migration rates, rates of sand supply or
757 loss are also important and may either augment or offset rate differences arising from variations
758 in sand supplied from the underlying substrate.

### 4.4 Substrate Slope Effects

The differently varying cross-shore substrate slopes associated with northern and southern Metompkin represent a major difference between the two island halves and strongly influence island behavior in both the late-Holocene and future simulations. At the beginning of the base simulations, neither island half is associated with a significant back-barrier deposit (Fig. 5). Were back-barrier sedimentation not to occur the island would initially adjust toward equilibrium with a shallower substrate slope only by increasing in height (i.e., in volume) (as in Wolinsky & Murray, 2009; Moore et al., 2010), which decreases average barrier island slope and results in a more landward migration trajectory. However, as our simulations progress forward in time, the existing back-barrier quickly widens and since back-barrier sedimentation keeps pace with sea-level rise (in the base simulations), the height of the island relative to the surface immediately behind it (now the surface of the marsh or lagoon) no longer changes (Fig. 6). In this case, the presence of a back-barrier deposit provides an elevated platform for the island to migrate onto, therefore allowing a stable vertical position relative to sea level to be achieved with less landward migration and a smaller island volume compared with instances in which a back-barrier deposit is absent. Because the shoreface depth and the height of the island relative to the surface of the back-barrier do not change, average barrier island slope cannot adjust. It follows, then, that for scenarios in which a back-barrier platform is present changes in barrier island volume and migration trajectory are less directly tied to the substrate slope than they are when back-barrier deposition is absent.

We explore the modulation of island adjustments to substrate slope by comparing island and back-barrier configurations resulting from RSLR scenarios (i.e. constant duration and future simulations) and evaluating how antecedent topography—both large-scale average slope and

782 short-term perturbations in substrate slope—influences island migration in the presence of back-
783 barrier deposition. In contrast to scenarios in which back-barrier deposition does not occur, the
784 migration trajectories (and therefore migration rates) observed within our simulations remain
785 relatively constant even when traversing substrates of locally varying slope early on in the
786 migration process (Figs. 6a, 6b, 13a, 13b). This suggests that when back-barrier deposition
787 persists at sufficiently high rates to keep up with RSLR, interactions between substrate slope and
788 back-barrier sedimentation will tend to allow the effect of local changes in slope to be
789 accommodated through changes in back-barrier width rather than directly through changes in
790 island migration trajectory/rate (as in the absence of a back-barrier deposit). When the substrate
791 slope is lower (higher) than the slope of the current island trajectory the back-barrier will widen
792 (become narrower) and therefore the resulting deposit will be thicker (thinner). This means that
793 the contact between the back-barrier unit and the unit below becomes deeper on the shoreface.
794 Subsequent effects on the migration trajectory, and therefore migration rates, only occur through
795 changes in shoreface sand content arising from such changes in back-barrier width and thickness.
796 The modulation of migration trajectories by back-barrier deposition suggests the
797 possibility for feedbacks to arise as the percentage of the shoreface consisting of back-barrier
798 deposit changes if the sand content of the back-barrier deposit differs from that of the
799 stratigraphic unit below. For cases in which the back-barrier width changes (because substrate
800 slope is different than the slope of the island trajectory) and the back-barrier deposit contains *less*
801 sand than the underlying unit (e.g., in the case of North Metompkin) a *negative* feedback
802 between back-barrier width and sand availability will tend to develop. In this case, sand
803 availability will decrease (increase) as the back-barrier thickens (narrows), resulting in increased
804 (decreased) island migration rates and therefore less (more) back-barrier expansion, leading to a

805 stable equilibrium back-barrier width (Table 3). In the case of this negative feedback, island
806 trajectories will tend to adjust to match average substrate slope (e.g., Fig. 13a)—as ultimately
807 occurs in the absence back-barrier deposition (Wolinsky & Murray, 2009; Moore et al., 2010).
808 When it occurs, the negative feedback described above will be reinforced by a secondary
809 feedback involving the contact between the back-barrier deposit and the barrier sands above.
810 This arises because, at each point in time, backbarrier deposits are emplaced immediately
811 landward of the island and thus, the slope of the contact between the island and back-barrier
812 deposits is determined by (and the same as) the migration trajectory. When the migration
813 trajectory changes because of changes in the thickness of the back-barrier unit, as described
814 above, the slope of the contact between the barrier and the back-barrier units changes. When the
815 slope of the contact becomes shallower (steeper), the seaward-edge of the contact between the
816 back-barrier deposits and island sand moves to a higher (lower) elevation, and thus the sandy
817 part of the island becomes thinner (thicker), leading to a smaller (larger) island. In both cases,
818 changes in effective island slope and migration trajectory that result from changes in substrate
819 slope (via back-barrier widths/thickness) are self-reinforcing: as the shoreface-substrate sand
820 content decreases (increases) due to a thickening back-barrier, the resulting decrease (increase)
821 in island volume leads to an even lower (greater) shoreface-substrate sand content because the
822 smaller (larger) barrier accounts for an even smaller (larger) portion of the substrate, leading to
823 an even shallower (steeper) migration trajectory. This feedback involving the contact between
824 the back-barrier and barrier island units strengthens the negative feedback (i.e., further constrains
825 variation in back-barrier width) that occurs when the back-barrier unit is less sandy than the unit
826 below.

827 Alternatively, if the back-barrier deposit contains more sand than the underlying unit
828 (e.g., southern Metompkin Island), a *positive* feedback will develop during back-barrier
829 expansion (contraction) in which overall sand availability increases (decreases) as the back-
830 barrier expands (contracts) and consequently the contact between the back-barrier and the
831 underlying unit becomes lower (higher) on the shoreface, allowing migration rates to decline
832 (increase) further (Table 3). The secondary feedback involving the contact between the back-
833 barrier unit and the barrier island unit strengthens the positive feedback in a similar way as
834 described in the case of the negative feedback above. In the case of the positive feedback, with
835 continued migration the back-barrier will grow indefinitely or disappear (e.g., Fig. 13b). With
836 continued migration, if the shoreface is entirely made up of sand-rich material (e.g., back-barrier
837 grows indefinitely), this self-reinforcing feedback would entirely decouple substrate slope and
838 the island migration trajectory. Only when high or low substrate slopes (relative to the current
839 migration trajectory) persist across a significant expanse will either positive feedback have the
840 potential to persist, leading to runaway back-barrier widening or narrowing. In addition,
841 prolonged widening of a sand-rich back-barrier implies a net input of sand to the island/back-
842 barrier system, and therefore is most likely when the back-barrier sand comes from fluvial
843 sources or coastal deposits other than the local island and shoreface (e.g. imported by tidal
844 currents from distal sources, or replenished by convergence of alongshore sediment transport).
845 Regardless of whether or not a runaway feedback occurs, changes in substrate slope that increase
846 or decrease the width of the back-barrier deposit will affect the thickness of the back-barrier
847 exposed on the shoreface after a time lag characterized by the width of the current back-barrier
848 divided by the current migration rate.
849

## 5. CONCLUSIONS

The results of our numerical experiments demonstrate that back-barrier sedimentation plays an important role determining the characteristics and behavior of barrier islands. Back-barrier environments producing relatively sand-rich deposits tend to result in barriers that have a large volume and relatively low rates of landward migration, and vice versa. In addition, our results demonstrate that back-barrier sedimentation fundamentally changes the way barrier islands evolve in response to rising sea level, relative to the case without back-barrier sedimentation. In the absence of back-barrier sedimentation, the slope of the landscape across which a barrier migrates (the 'substrate slope') directly influences barrier island volume and migration rate. In contrast, when a back-barrier environment is present, the influence of substrate slope becomes indirect and time lagged.

Low substrate slopes landward of the back-barrier environment, relative to the slope of the present barrier-island trajectory (the ratio between the RSLR rate and the rate of landward barrier migration), tend to produce widening of the back-barrier environment, and therefore eventually to thickening of the back-barrier deposit that the barrier migrates over (and vice versa). Depending on whether the back-barrier deposit is more or less sand rich than the underlying substrate, changes in back-barrier width caused by changes in the slope of the substrate can lead to either a negative or a positive feedback. When the back-barrier deposit is relatively sand poor (e.g. marsh deposits), a negative feedback arises; low landward slopes and associated back-barrier widening tend to cause increases in barrier migration rate (and vice versa), buffering back-barrier width changes. In this case, temporal fluctuations in substrate slope will only produce small fluctuations about a stable back-barrier width. However, relatively sand-rich back-barrier deposits (e.g. from an open bay environment) tend to produce a positive

feedback; low landward slopes and associated back-barrier widening/thickening tend to cause decreases in migration rate, which then reinforce back-barrier widening. (The reverse is true: relatively steep landward slopes and associated back-barrier narrowing/thinning tend to cause increases in migration rates and therefore reinforce narrowing/thinning). Thus, back-barrier environments that produce sand-rich deposits will tend to disappear or to widen indefinitely (although indefinite widening will only occur given a sufficient influx of sand from fluvial or alongshore sources).

## ACKNOWLEDGEMENTS

Funding was provided by the Virginia Coast Reserve Long-Term Ecological Research Program (National Science Foundation DEB-123773), the Department of Environmental Sciences at the University of Virginia and the Geomorphology and Land use Dynamics Program of the National Science Foundation (EAR-1324973). We thank Pat Wiberg and Alan Howard for their helpful comments on an earlier version of this manuscript. We thank Kiki Patsch and Jeff List for assistance with coding and determination of average bathymetric profiles, respectively. We also thank Editor Andy Plater, Andrew Green and an anonymous reviewer for helpful feedback that improved this manuscript.

## FIGURE & TABLE CAPTIONS

Table 1. Model input values from base simulations representing average values during late-Holocene, and range of values tested within sensitivity analyses. B.I. = barrier island; BB = backbarrier; strat 1 =early Holocene lagoonal unit; strat 2 = sand-rich late Pleistocene unit.

Table 2. Average migration rate (m/yr) and volume change (initial subtracted from final in $m^3/m$) of all RSLR rate scenarios when total RSLR is 1 m and 1.6 m RSLR for northern and southern Metompkin Island.

Figure 1. a) Location of the Delmarva Penninsual along U.S. mid-Atlantic coastline. b) The southern Delmarva Peninsula, including mainland, marsh, and barrier islands. The box delineates Metompkin Island. c) Image of Metompkin Island, VA (2007, from Google Earth) showing the current ~200 m mid-island shoreline offset co-located with the mid-island shift in back-barrier environment. Northern Metompkin is backed by a nearly continous platform marsh, while southern Metompkin Island is backed by a narrow, fringing marsh and a shallow open lagoon.

Figure 2. a) Approximate Metompkin Island shoreline position before and after breaching of ephemeral inlet in 1957. b) Rapid island migration, additional island breeching and shoreface erosion during 1962 storm, results in a prominent mid-island offset by 1981 (Modified from Byrnes, 1988).

Figure 3. GEOMBEST simulates the evolution of three functional realms (back-barrier, barrier, shoreface) and three primary stratigraphic units (back-barrier deposits, barrier island and underlying strata). The relationship between the average slope of the barrier island and the average slope of the underlying substrate is important in determining the island migration rate and trajectory during transgression (Modified from Moore et al., 2010).

Figure 4. Representation of the average modern morphology and stratigraphy of northern (a) and southern (b) Metompkin Island derived from bathymetric data and published core findings. (Yellow/light gray stratigraphic unit represents barrier island sand, dark gray represents marsh (a) or lagoonal (b) deposits, and tan/medium gray units represent underlying stratigraphic layers.)

Figure 5. Plausible initial (~4600 yr bp) morphology and stratigraphy representing average conditions for northern (a) and southern (b) Metompkin Island, developed based on available geological and geophysical data.

Figure 6. Final stratigraphy and morphology of (a) northern and (b) southern Metompkin Island for late-Holocene sensitivity experiment simulations in which RSLR rate is set to 4 mm/yr. Ghost traces (one every 400 years, except last increment, which represents 200 years) depict island position through time.

Figure 7. Initial (~4600 yr bp), model-generated, final (~1950) and modern (~2005) morphologies resulting from calibration of northern (a) and southern (b) Metompkin Island base simulations. Black line indicates actual modern surface derived from averaging of topographic and bathymetric data. The offshore position of the model-generated surface relative to the modern surface occurs because of the time difference between the two. As described in section 2.2 we adjusted input parameters within published ranges to reproduce the ~1950 (prior to breaching of the island in 1957 and the consequent development of the mid-island offset) shoreline position.

942 Figure 8. Sensitivity of island migartion rate to changes in backbarrier sedimentation rate (a),
943 sand-supply rate (b), depth-dependent reponse rate (DDRR) (c), shoreface depth (d) and RSLR
944 rate (e,f) for northern and southern Metompkin Island. Shaded region denotes parameter value
945 from base simulation.
946
947 Figure 9. Sensitivity of island volume to changes in backbarrier sedimentation rate (a), sand-
948 supply rate (b), depth-dependent reponse rate (DDRR) (c), shoreface depth (d) and RSLR rate
949 (e,f) for northern and southern Metompkin Island. Shaded region denotes parameter value from
950 base simulation.
951
952 Figure 10. Sensitivity of average island migration rate (left panels) and final island volume
953 (right panels) to fluctuations in the sand content of each stratigraphic unit for northern (top
954 panels) and southern (bottom panels) Metompkin Island.
955
956 Figure 11. Sensitivity of average island migration rate (left panels) and final island volume
957 (right panels) to fluctuations in the erodibility of each stratigraphic unit for northern (top panels)
958 and southern (bottom panels) Metompkin Island. See text (section 3.1.4) for a description of the
959 erodibility index.
960
961 Figure 12. a) Changes in back-barrier width (solid lines) with landward substrate slope (dashed
962 lines) during late-Holocene RSLR rate sensitivity simulations shown above. b) Final island
963 volume (dashed lines) compared to back-barrier width (solid lines) during late-Holocene RSLR
964 rate sensitivity simulations below (b).
965

966 Figure 13. Final stratigraphy and morphology of (a) northern and (b) southern Metompkin
967 Island for late-Holocene sensitivity experiment simulations in which RSLR rate is set to 4
968 mm/yr. Ghost traces (one every 400 years, except last increment, which represents 200 years)
969 depict island position through time.
970
971 Figure 14. Final stratigraphy and morphology of (a) northern and (b) southern Metompkin Island
972 for a future simulation (starting from the modern configuration shown in Figure 4) in which
973 RSLR rate increase linearly from 4 mm/yr to a total RSLR of 1 m after 100 years (~2100 AD).
974 Ghost traces (one every ~15 years, except last increment, which represents 10 years) depict
975 island position through time.
976
977 Figure 15. Average island migration rates (a) and final island volume (b) for future simulations
978 of northern (solid lines) and southern (dashed lines) Metompkin Island for in which RSLR rates
979 are constant, linearly increasing, or polynomially increasing and for simulations in which back-
980 barrier sedimentation rate is limited to 10 mm/yr with and without a 20-year lag.
981
982 Figure 16. Shoreface-substrate sand content (% of total volume) of stratigraphic units exposed
983 along the active shoreface over the duration of the late-Holocene base simulations.
984
985 **REFERENCES**

986 Bruun, P., 1962. Sea-level rise as cause of coastal erosion. Journal of the Waterways and Harbor
987 Division, ASCE 88, 117-130.

988 Byrne, R.J., Dealteris, J.T., Bullock, P.A., 1974. Channel stability in tidal inlets: A case study.
989 Proceedings from the 14th Coastal Engineering Conference, ASCE, New York, 1585-
990 1604.
991 Byrnes, M.R., 1988. Holocene geology and migration of a low-profile barrier island system,
992 Metompkin Island, Virginia. Ph.D. Thesis, Old Dominion University.
993 Cooper, J.A.G, 1994. Lagoons and Microtidal Coasts In: Carter, R. W. G., Woodroff, C. D.
994 (Eds.), Coastal Evolution: Late Quaternary Shoreline Morphodynamics. Press Syndicate
995 of the University of Cambridge, UK, 219-266.
996 Cowell, P.J., Roy, P.S., Jones, R.A., 1995. Simulation of large-scale coastal change using a
997 morphological behavior model. Marine Geology 126, 45-61.
998 Craft,C., Clough, J., Ehman, J., Joye, S., Park, R., Pennings, S., Guo, H., Machmuller, M., 2009.
999 Forecasting the effects of accelerated sea-level rise on tidal marsh ecosystem services.
1000 Front. Ecol. Environ. 7, 73-78.
1001 Curray, J.R., 1964. Transgressions and regressions. In: Miller, R.L. (Ed.), Papers in Marine
1002 Geology. Macmillan, New York, NY, 175-203.
1003 Demarest, J.M., Leatherman, S.P., 1985. Mainland influence on coastal transgression: Delmarva
1004 Peninsula. Marine Geology 63, 19-33.
1005 Ellis, J., Stone, G.W., 2006. Numerical simulation of net longshore sediment transport and
1006 granulometry of surficial sediments along Chandeleur Island, Louisiana, USA. Marine
1007 Geology 232 (3), 115-129.
1008 Engelhart, S.E., Horton, B.P., Douglas, B.C., Peltier, W.R., Tornqvist, T.E., 2009. Spatial
1009 variability of late Holocene and 20th century sea-level rise along the Atlantic coast of the
1010 United States. Geology 37 (12), 1115-1118.

1011 Everts, C.H., 1978. Geometry of profiles across inner continental shelves of the Atlantic and gulf
1012 coasts of the United States. Fort Belvoir, Va.: U.S. Army Corps of Engineers, Coastal
1013 Research Center.
1014 Finkelstein, K.H., 1986. Backbarrier contributions to a littoral sand budget, Virginia eastern
1015 shore, USA. Journal of Coastal Research 2 (1), 33-42.
1016 Finkelstein, K.H., Ferland, M.A. (Eds.), 1987. Back-barrier response to sea-level rise, eastern
1017 shore of Virginia, 41st ed. Special Publications: The Society of Economic Paleontologists
1018 and Mineralogists.
1019 Foyle, A.M., Oertel, G.F., 1997. Transgressive systems tract development and incised-valley fills
1020 within a quaternary estuary-shelf system; Virginia inner shelf, USA. Marine Geology 137
1021 (3-4), 227.
1022 Green, A.N., Cooper, A.G., Salzmann, L., 2014. Geomorphic and stratigraphic signals of
1023 postglacial meltwater pulses on continental shelves. Geology 42 (2), 151-154.
1024 Grinsted, A., Moore, J.C., Jeverjeva, S., 2009. Reconstructing sea level from paleo and projected
1025 temperatures 200 to 2100 AD. Climate Dynamics 34 (4) 461-472.
1026 Gutierrez, B.T., Williams, S.J., Thieler, E.R., 2007. Potential for shoreline changes due to sea-
1027 level rise along the U.S. mid-Atlantic region. United States Geological Survey Report
1028 Series, 1278.
1029 Halsey, S. A. 1979. Nexus: New model of barrier island development. In: Leatherman, S.P.
1030 (Ed.), Barrier Islands from the Gulf of St. Lawrence to the Gulf of Mexico. Academic
1031 Press, New York, 185-210.

1032 Hayden, B.P., Dolan, R., Ross, P., 1980. Barrier island migration; thresholds in geomorphology.
1033 In: Coates, D.R., Vitek, J.D. (Eds.), Thresholds in geomorphology. George Allen &
1034 Unwin, London, UK, 363-384.
1035 Jevrejeva, S., Moore, J.C., Grinsted, A., 2010. How will sea level respond to changes in natural
1036 and anthropogenic forcings by 2100? Geophyscial Research Letters 37, L07703.
1037 IPCC, 2013. Climate Change 2013: Impacts, Adaptation and Vulnerability: Contributions of
1038 Working Group II to the Fifth Assessment Report of the Intergovernmental Panel on
1039 Climate Change, Cambridge University Press, New York, NY.
1040 Kirwan, M.L., Guntenspergen, G.R., D'Alpaos, A., Morris, J.T., Mudd, S.M., Temmerman, S.,
1041 2010. Limits on the adaptability of coastal marshes to rising sea level. Geophysical
1042 Research Letters 37, L23401.
1043 Kirwan, M.L., Temmerman, S., 2009. Coastal marsh response to historical and future sea-level
1044 acceleration. Quarternary Science Reviews 28 (17), 1801-1808.
1045 Knutson, T.R., Mcbride, J., Chan, J., Emanuel, K., Holland, G., Landsea, C., Held, I., Kossin,
1046 J.P., Srivastava, A.K., Sugi, M., 2010. Tropical cyclones and climate change. Nature 3
1047 157-163. doi: 10.1038/ngeo779.
1048 Larson, M., 1991. Equilibrium profile of a beach with varying grain size. Coastal Sediments.
1049 ASCE-1991, 905-919.
1050 Leatherman, S.P., Rice, T.E., Goldsmith, V., 1982. Virginia Barrier Island Configuration: A
1051 Reappraisal. Science 215 (4530), 285-287.
1052 McBride, R.A., Moslow, T.F., 1991. Origin, evolution, and distribution of shoreface sand ridges,
1053 Atlantic inner shelf, U.S.A. Marine Geology 97, 57-85. McNamara, D., Werner, B.T.,
1054 2008. Coupled barrier island–resort model: 1. Emergent instabilities induced by strong

1055 human-landscape interactions. Journal of Geophysical Research-Earth Surface. 113 (F01)
1056 doi: 10.1029/2007JF000840.
1057 Mellett, C.L., Hodgson, D.M., Lang, A., Mauz, B., Selby, I., Plater, A.J., 2012. Preservation of a
1058 drowned gravel barrier complex: A landscape evolution study from the north-eastern
1059 English Channel. Marine Geology 315-318, 115-131.
1060 Mixon, R.B., 1985. Stratigraphic and geomorphic framework of uppermost Cenozoic deposits in
1061 the southern Delmarva Peninsula, Virginia and Maryland, U.S. U.S. Geological Survey
1062 Professional Paper 1067-G, 53p.
1063 Moore, L.J., List, J.H., Williams, S.J., Stolper, D., 2010. Complexities in barrier island response
1064 to sea level rise: Insights from numerical model experiments, North Carolina outer banks.
1065 Journal of Geophysical Research 115, 27.
1066 Moore, L.J., Patsch, K., Williams, S.J., List, J.L., 2014, Barrier Islands Poised for
1067 Geomorphic Threshold Crossing in Response to Rapid Sea-Level Rise: Insights from
1068 Numerical Model Experiments, Chandeleur Islands, Louisiana, USA. Marine Geology,
1069 355, 244-259. doi: 10.1016/j.margeo.2014.05.022
1070 Newman, W.S., Rusnak, G.A., 1965. Holocene submergence of the eastern shore of Virginia.
1071 Science 148 (3678), 1464-1466. doi: 10.1126/science.148.3676.1464
1072 Newman, W.S., Munsart, C.A, 1968. Holocene Geology of the Wachapreague Lagoon, Eastern
1073 Shore Peninsula, Virginia. Marine Geology 6(2), 81-105.
1074 Nichols, M. M., 1989. Sediment accumulation rates and relative sea-level rise in lagoons.
1075 Marine Geology, 88, 201-219.
1076 Nicholls, R. J., Birkemeir, W., Lee, G., 1998. Evaluation of depth of closure using data from
1077 Duck, NC, USA, Marine Geology, 148, 179-201. doi:10.1016/S0025-3227(98)00011-5.

1078 Oertel, G.F., Allen, T.R., Foyle, A.M., 2008. The influence of drainage hierarchy on pathways of
1079 barrier retreat; an example from Chincoteague Bight, Virginia, U.S.A. Southeastern
1080 Geology 45 (3), 179-201. Oertel, G. F., Kraft. J. C., 1994. New Jersey and Delmarva
1081 barrier islands. In: R. Davis (Ed.) Geology of Barrier Islands. Springer-Verlag,
1082 Heidelbeg, Germany, 207-226.
1083 Oertel, G.F., Woo, H.J., 1994. Landscape classification and terminology for marsh in deficit
1084 coastal lagoons. Journal of Coastal Research 10 (4), 919-932.
1085 Pilkey, O.H., Young, R.S., Bush, D.M., 2000. Comment on sea level rise shown to drive coastal
1086 erosion. EOS Transactions 81 (38), 437-441.
1087 Rice, T.E., Leatherman, S.P., 1983. Barrier island dynamics; the eastern shore of Virginia.
1088 Southeastern Geology 24 (3), 125-137.
1089 Sallenger, A.H., 2000. Storm impacts scale for barrier islands. Journal of Coastal Research 16
1090 (3), 890-895.
1091 Stolper, D., List, J.H., Thieler, E.R., 2005. Simulating the evolution of coastal morphology and
1092 stratigraphy with a new morphological-behavior model (GEOMBEST). Marine Geology
1093 218, 17-36.
1094 Stutz, M.L., Pilkey, O.H., 2011. Open-Ocean Barrier Islands: Global Influence of
1095 Climatic, Oceanographic, and Depositional Settings. Journal of Coastal Research 272,
1096 207-222.
1097 Van de Plassche, O., 1990. Mid-Holocene sea-level change on the eastern shore of Virginia.
1098 Marine Geology 91 (1-2), 149-154.
1099 Walters, D., Moore, L.J., Duran, O., Fagherazzi, S., Mariotti, G., 2014. Interactions
1100 between barrier islands and backbarrier marshes affect island system response to sea level

1101 rise: Insights from a coupled model. Journal of Geophysical Research—Earth Surface
1102 119, 2013-2031. DOI: 10.1002/2014JF003091.

1103 Wolinsky, M.A., Murray, A.B., 2009. A unifying framework for shoreline migration: 2.
1104 Application to wave-dominated coasts, Journal of Geophysical Research 114, 1–13,
1105 doi:10.1029/2007JF000856.

1106 Wolner, C.W.V., 2011. Ecomorphodynamic feedbacks and barrier island evolution, Virginia
1107 Coast Reserve, USA. Master's Thesis, University of Virginia, Charlottesville, VA, USA.

1108 Wolner, C.V., Moore, L.J., Young, D.R., Brantley, S.T., Bissett, S.N., McBride, R.A., 2013.
1109 Ecomorphodynamic feedbacks and barrier island response to disturbance: Insights from
1110 the Virginia Barrier Islands, Mid-Atlantic Bight, USA, Geomorphology 199, 115-128,
1111 doi:10.1016/j.geomorph.2013.03.035.

**FIGURES AND TABLES**

Table 1

| Parameter | | Calibration Value | | Source(s) | Sensitivity Variation |
|---|---|---|---|---|---|
| | | *North* | *South* | | |
| Stratigraphy | | | | Finkelstein & Ferland, 1987; Byrnes, 1988 | N/A |
| Initial Island Position | | 4km offshore | | Finkelstein & Ferland, 1987; Byrnes, 1988 | N/A |
| RSLRR | | 1.44mm/yr | | Newman & Rusnack, 1965; Finkelstein & Ferland, 1987; Byrnes, 1988 | 0.5 – 4mm/yr |
| Shoreface Depth | | 6.5m | | Everts, 1978 | 4 – 9m |
| Sand Comp. (% of total) | B.I. | 95 | 95 | Mixon, 1985; Finkelstein & Ferland, 1987; Byrnes, 1988; | 10-90% for all units |
| | BB | 15 (marsh) | 60 (lagoon) | | |
| | Strat1 | 20 | 20 | | |
| | Strat2 | 75 | 75 | | |
| Sand-supply Rate | | -0.5 $m^3$/m/yr | | US ACE, 1973; Byrne et. al, 1974; Byrnes, 1988 | -2 – 2 $m^3$/m/yr |
| Backbarrier Sedimentation Rate | | 1.44mm/yr | | Nichols, 1989; Van de Plassche, 1990 | 0 – 2.5mm/yr |
| Erodibility | | 1 | 1 | Moore et al., 2010 | .001-1 |
| DDRR | | 1 | | Moore et al., 2010 | .001 – 1 |
| Max. Backbarrier Elevation | | 0.35m | -0.4m | modern morphology | n/a |

Table 2

| | 1m RSLR | | 1.6m RSLR | |
|---|---|---|---|---|
| | Migration Rate (m/yr) | Volume Increase ($m^3/m$) | Migration Rate (m/yr) | Volume Increase ($m^3/m$) |
| North | 1.02 | 726 | 1.31 | 851 |
| South | 0.55 | 309 | 0.88 | 549 |

Table 3

| | Backbarrier sand content < unit below (e.g., N. Metompkin) = Negative Feedback | | | Backbarrier sand content > unit below (e.g., S. Metompkin) = Positive Feedback | | |
|---|---|---|---|---|---|---|
| | Shoreface Sand % | Migration Rate | Island Volume | Shoreface Sand % | Migration Rate | Island Volume |
| Gentle slope → Increase in Backbarrier Thickness | ↓ | ↑ | ↓ | ↑ | ↓ | ↑ |
| Steep slope → Decrease in Backbarrier Thickness | ↑ | ↓ | ↑ | ↓ | ↑ | ↓ |

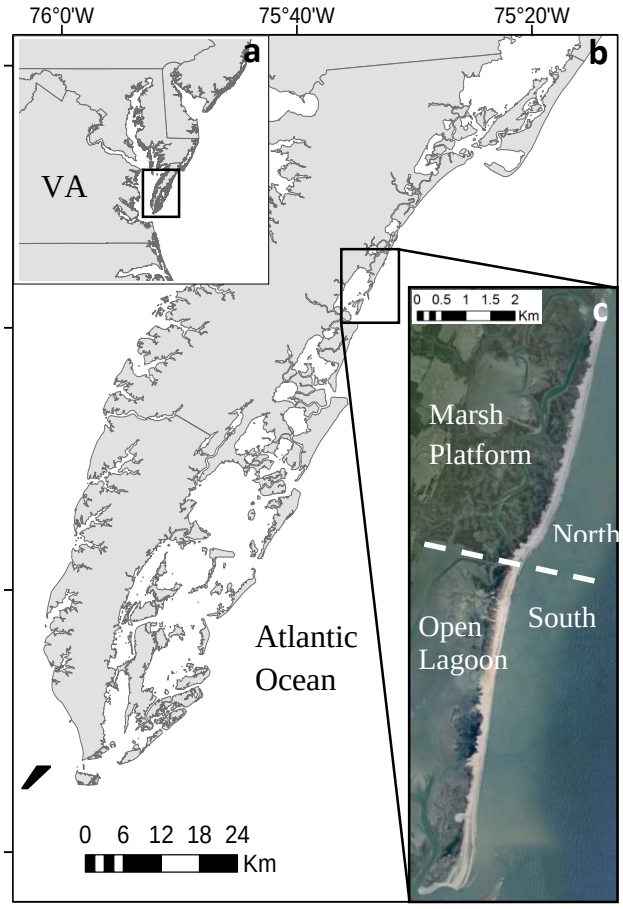
76°0'W
75°40'W
75°20'W
a
b
VA
0 0.5 1 1.5 2
Km
c
Marsh
Platform
North
South
Open
Lagoon
Atlantic
Ocean
0 6 12 18 24
Km

Figure 1

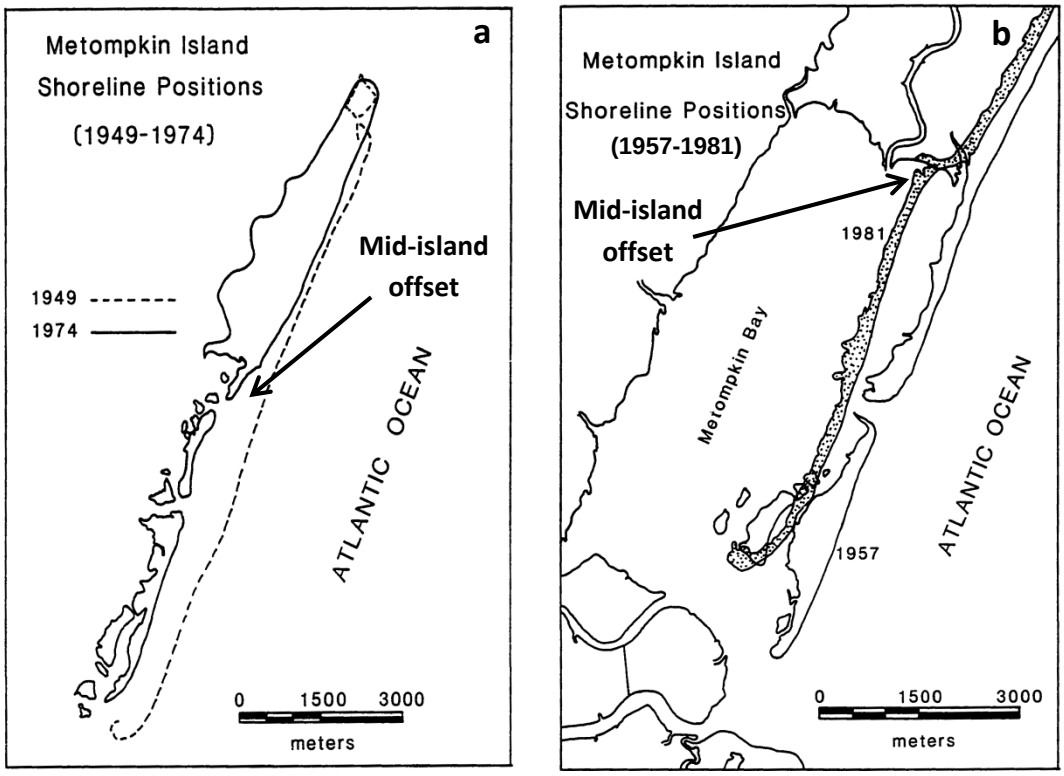


Figure 2

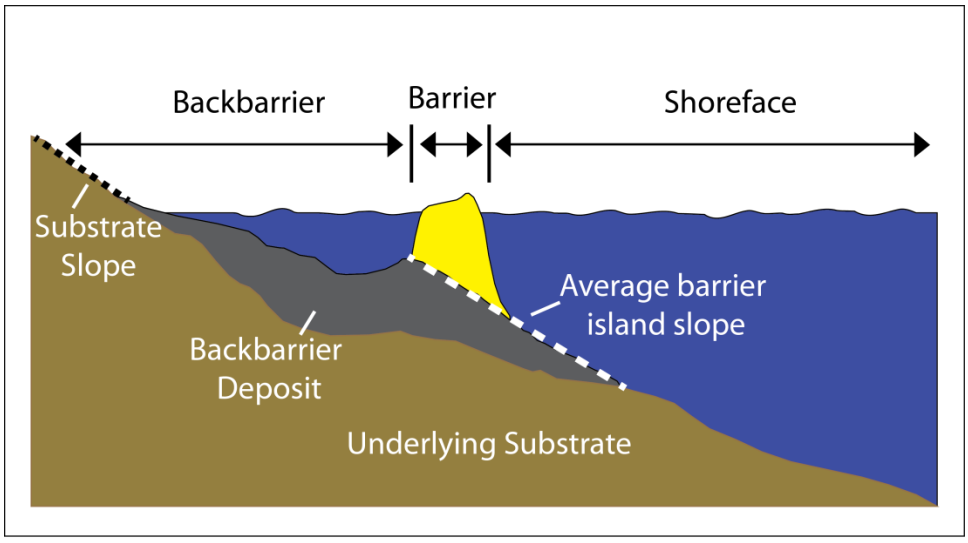


Figure 3

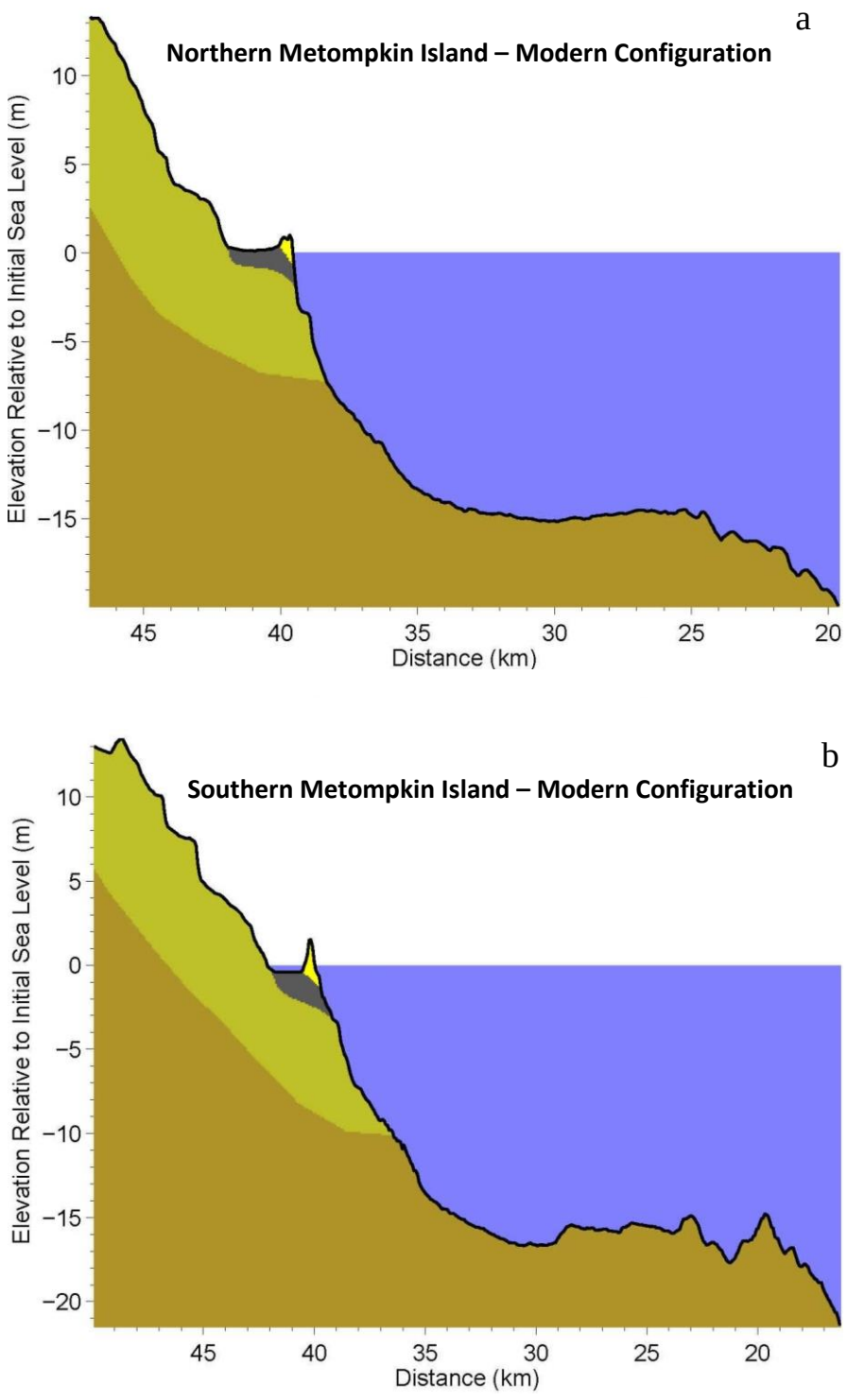
a
Northern Metompkin Island – Modern Configuration
Elevation Relative to Initial Sea Level (m)
10
5
0
−5
−10
−15
45
40
35
30
25
20
Distance (km)
b
Southern Metompkin Island – Modern Configuration
Elevation Relative to Initial Sea Level (m)
10
5
0
−5
−10
−15
−20
45
40
35
30
25
20
Distance (km)

Figure 4

a

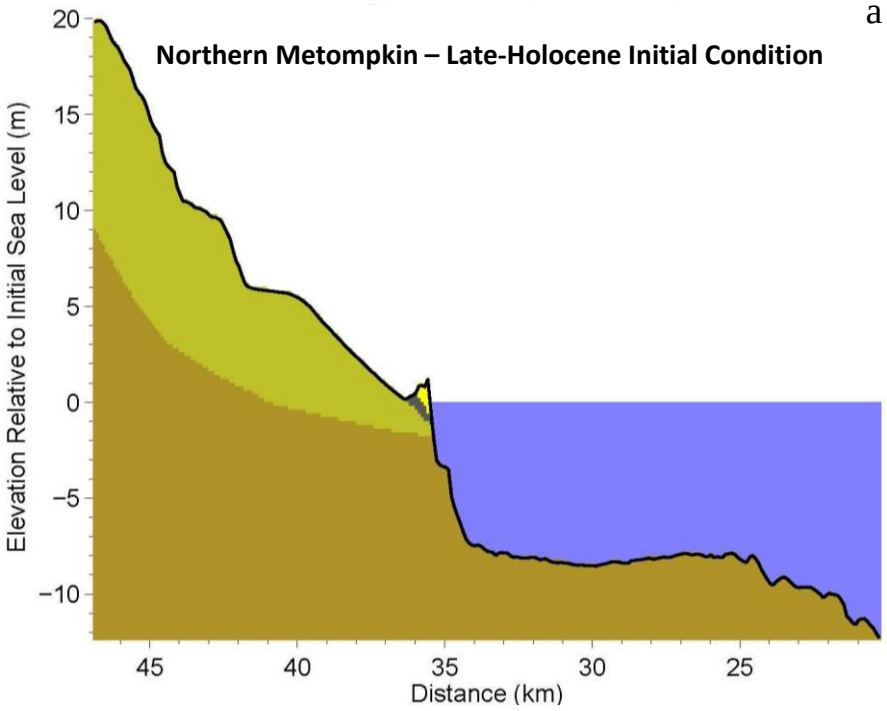
Northern Metompkin – Late-Holocene Initial Condition
Elevation Relative to Initial Sea Level (m)
20
15
10
5
0
−5
−10
45
40
35
30
25
Distance (km)

b

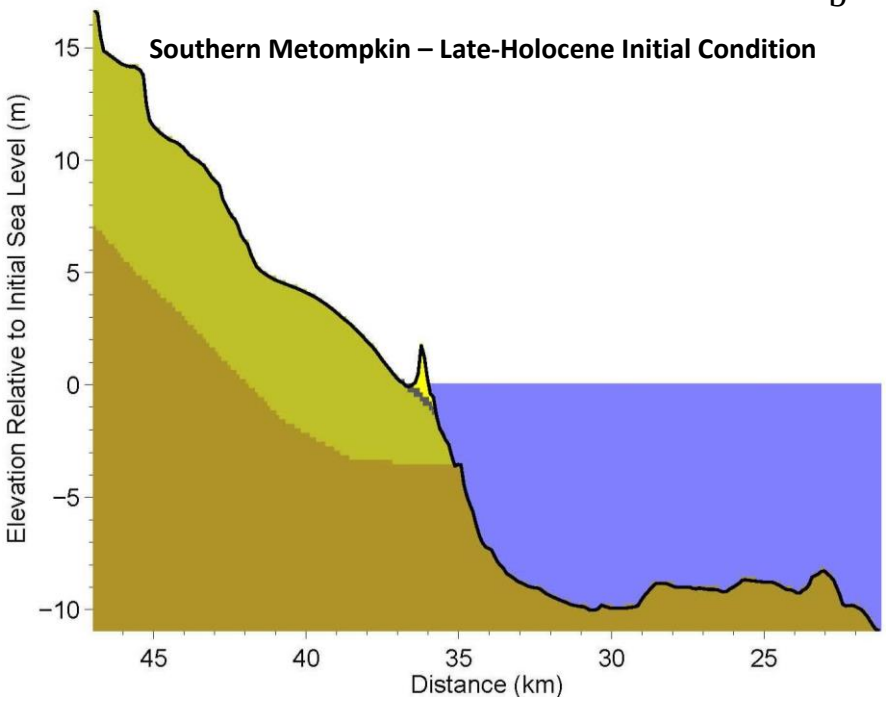
Southern Metompkin – Late-Holocene Initial Condition
Elevation Relative to Initial Sea Level (m)
15
10
5
0
−5
−10
45
40
35
30
25
Distance (km)

Figure 5

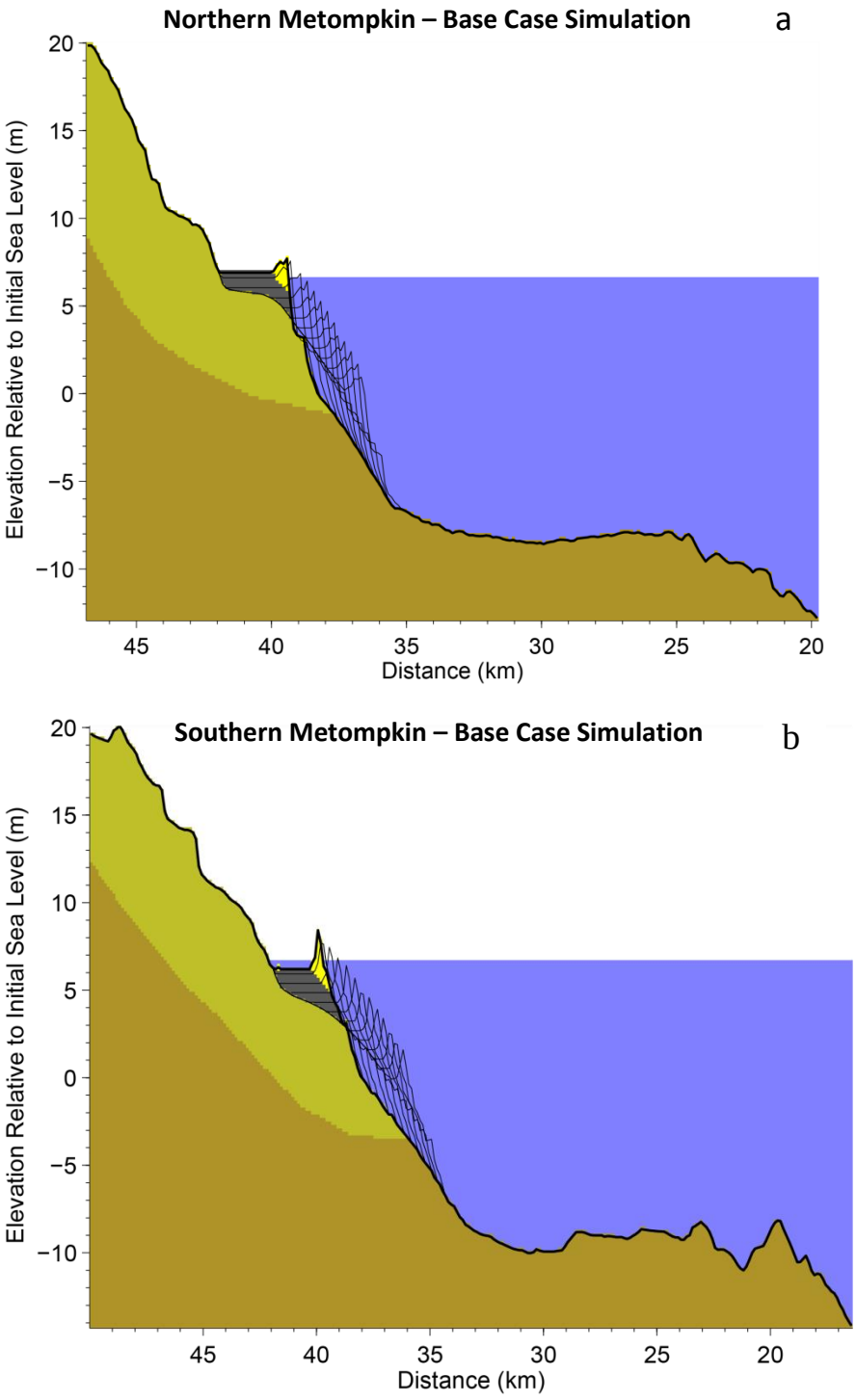
Northern Metompkin – Base Case Simulation
a
Elevation Relative to Initial Sea Level (m)
20
15
10
5
0
−5
−10
45
40
35
30
25
20
Distance (km)
Southern Metompkin – Base Case Simulation
b
Elevation Relative to Initial Sea Level (m)
20
15
10
5
0
−5
−10
45
40
35
30
25
20
Distance (km)

Figure 6

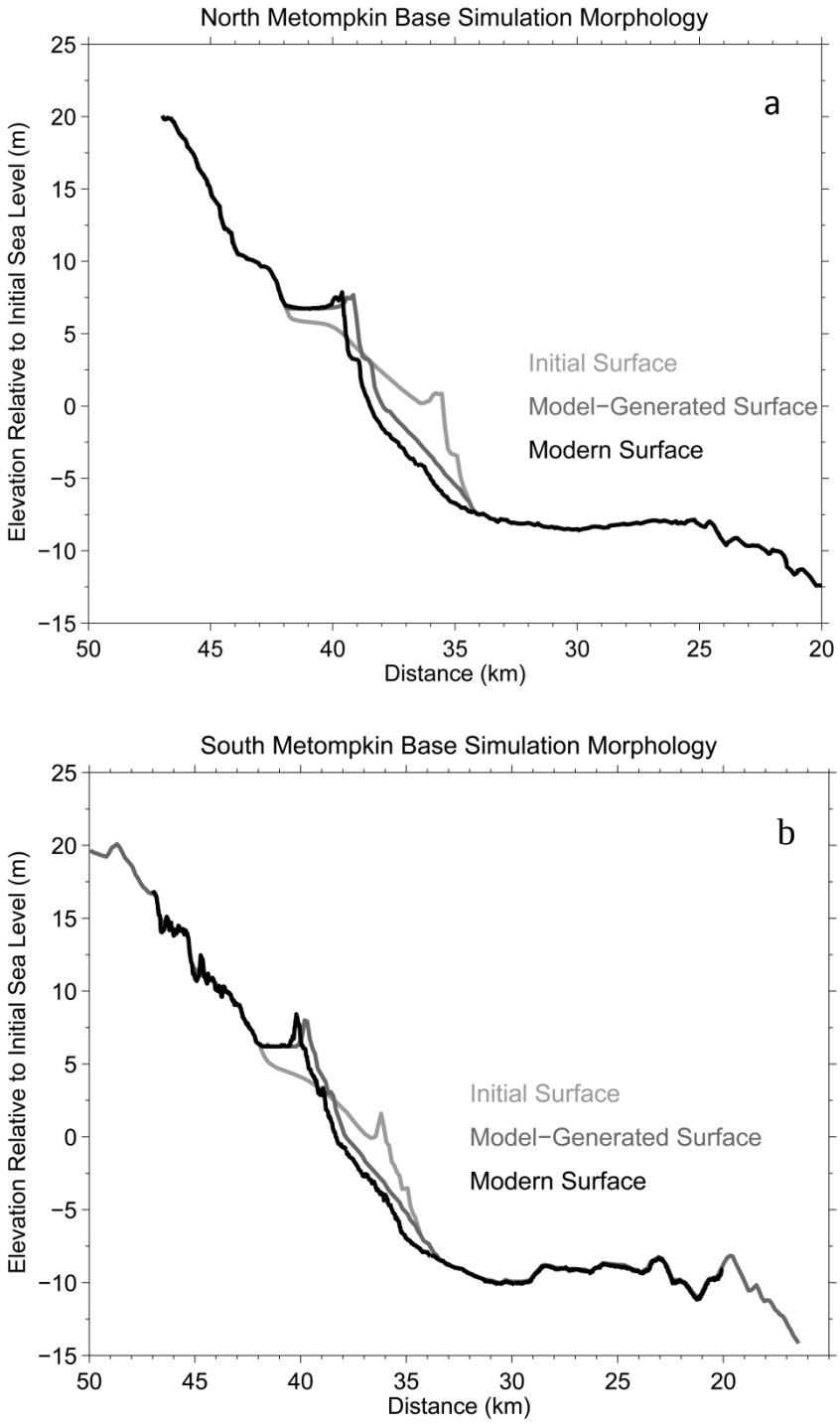
North Metompkin Base Simulation Morphology
a
Initial Surface
Model−Generated Surface
Modern Surface
Elevation Relative to Initial Sea Level (m)
Distance (km)
South Metompkin Base Simulation Morphology
b
Initial Surface
Model−Generated Surface
Modern Surface
Elevation Relative to Initial Sea Level (m)
Distance (km)

Figure 7

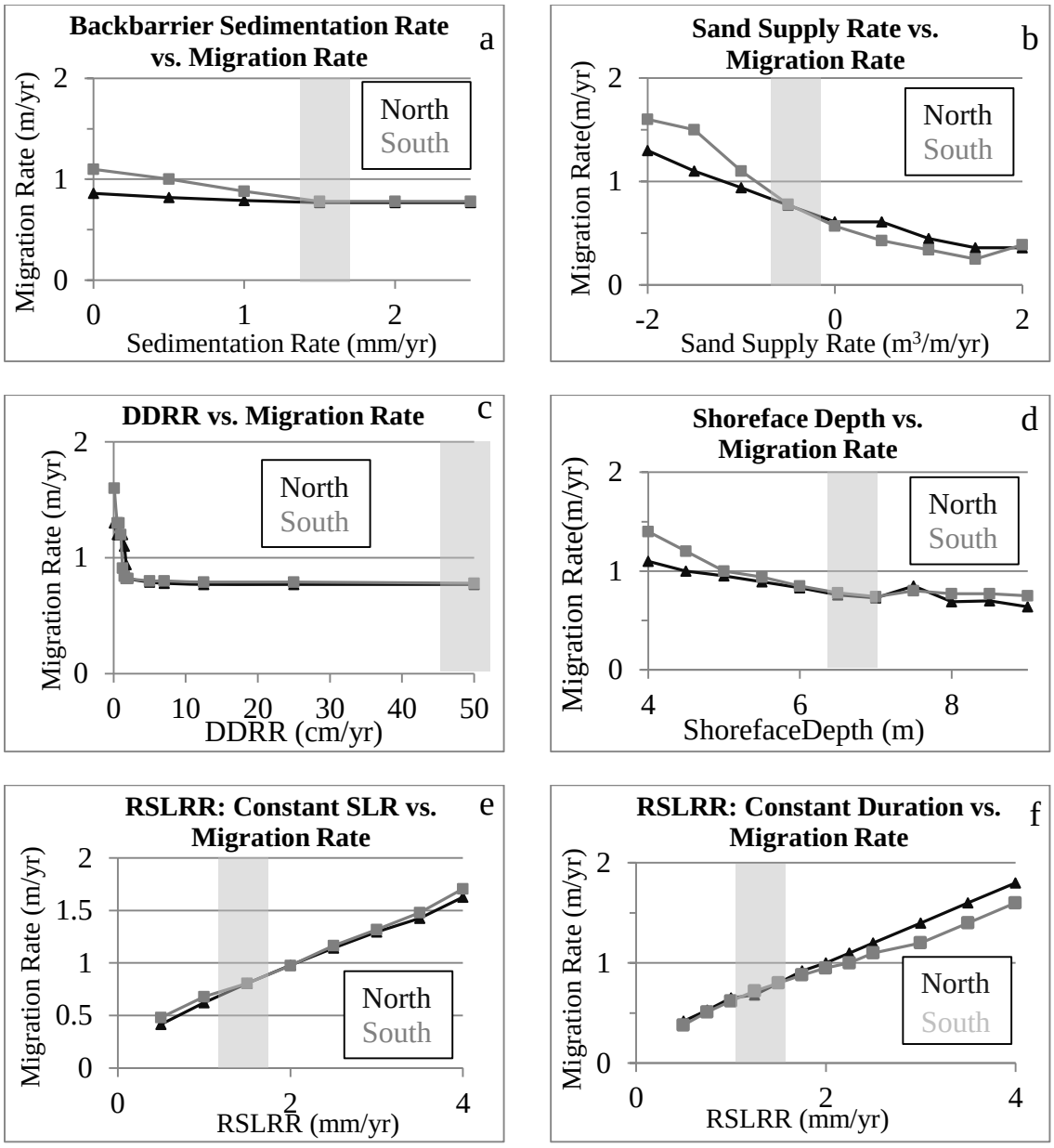
Backbarrier Sedimentation Rate vs. Migration Rate
a
Migration Rate (m/yr)
Sedimentation Rate (mm/yr)
North
South
Sand Supply Rate vs. Migration Rate
b
Migration Rate(m/yr)
Sand Supply Rate (m3/m/yr)
DDRR vs. Migration Rate
c
DDRR (cm/yr)
Shoreface Depth vs. Migration Rate
d
ShorefaceDepth (m)
RSLRR: Constant SLR vs. Migration Rate
e
RSLRR (mm/yr)
RSLRR: Constant Duration vs. Migration Rate
f

Figure 8

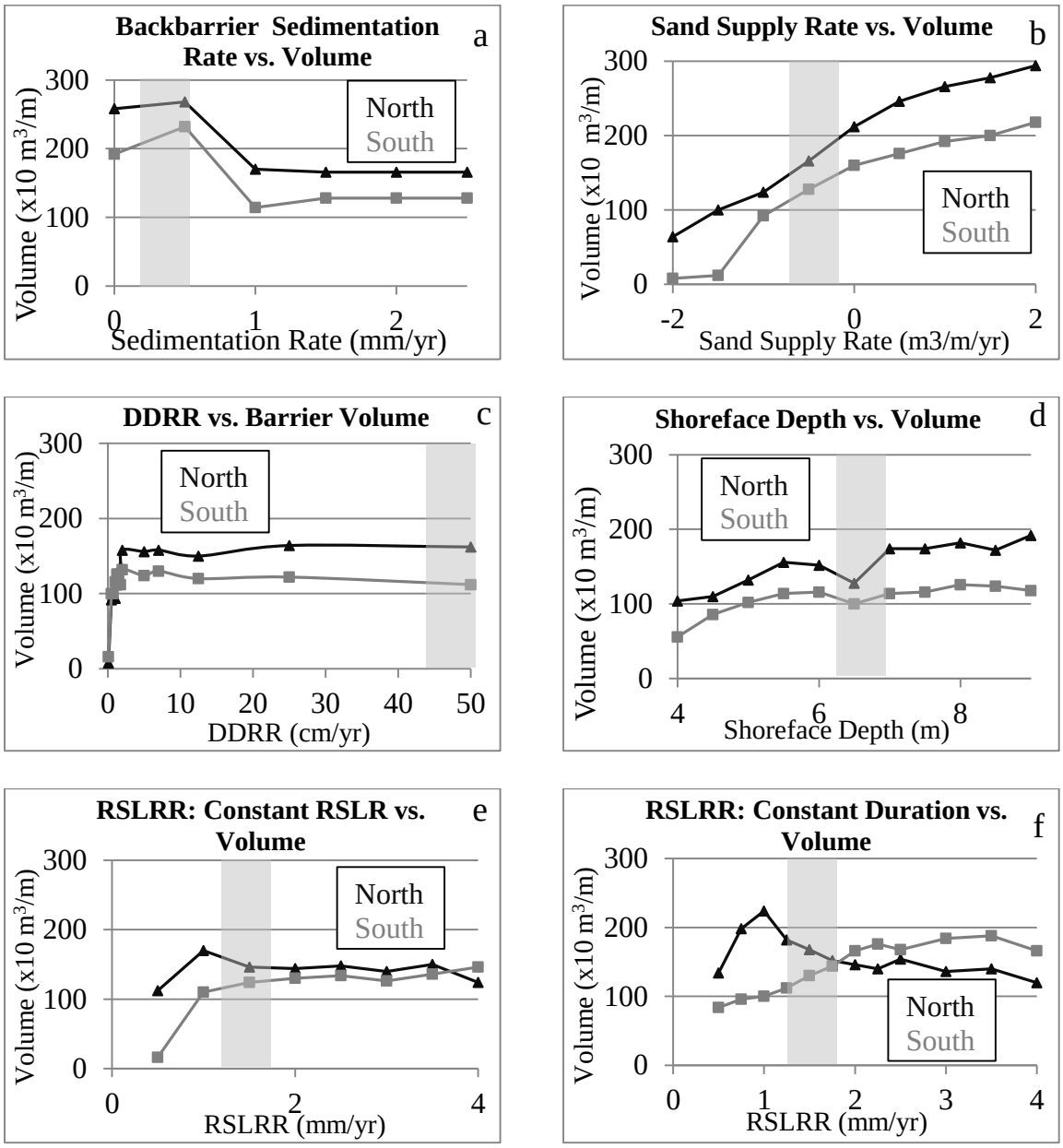
Backbarrier Sedimentation Rate vs. Volume
a
Volume (x10 m3/m)
300
200
100
0
0
1
2
Sedimentation Rate (mm/yr)
North
South
Sand Supply Rate vs. Volume
b
Volume (x10 m3/m)
300
200
100
0
-2
0
2
Sand Supply Rate (m3/m/yr)
North
South
DDRR vs. Barrier Volume
c
Volume (x10 m3/m)
300
200
100
0
0
10
20
30
40
50
DDRR (cm/yr)
North
South
Shoreface Depth vs. Volume
d
Volume (x10 m3/m)
300
200
100
0
4
6
8
Shoreface Depth (m)
North
South
RSLRR: Constant RSLR vs. Volume
e
Volume (x10 m3/m)
300
200
100
0
0
2
4
RSLRR (mm/yr)
North
South
RSLRR: Constant Duration vs. Volume
f
Volume (x10 m3/m)
300
200
100
0
0
1
2
3
4
RSLRR (mm/yr)
North
South

Figure 9

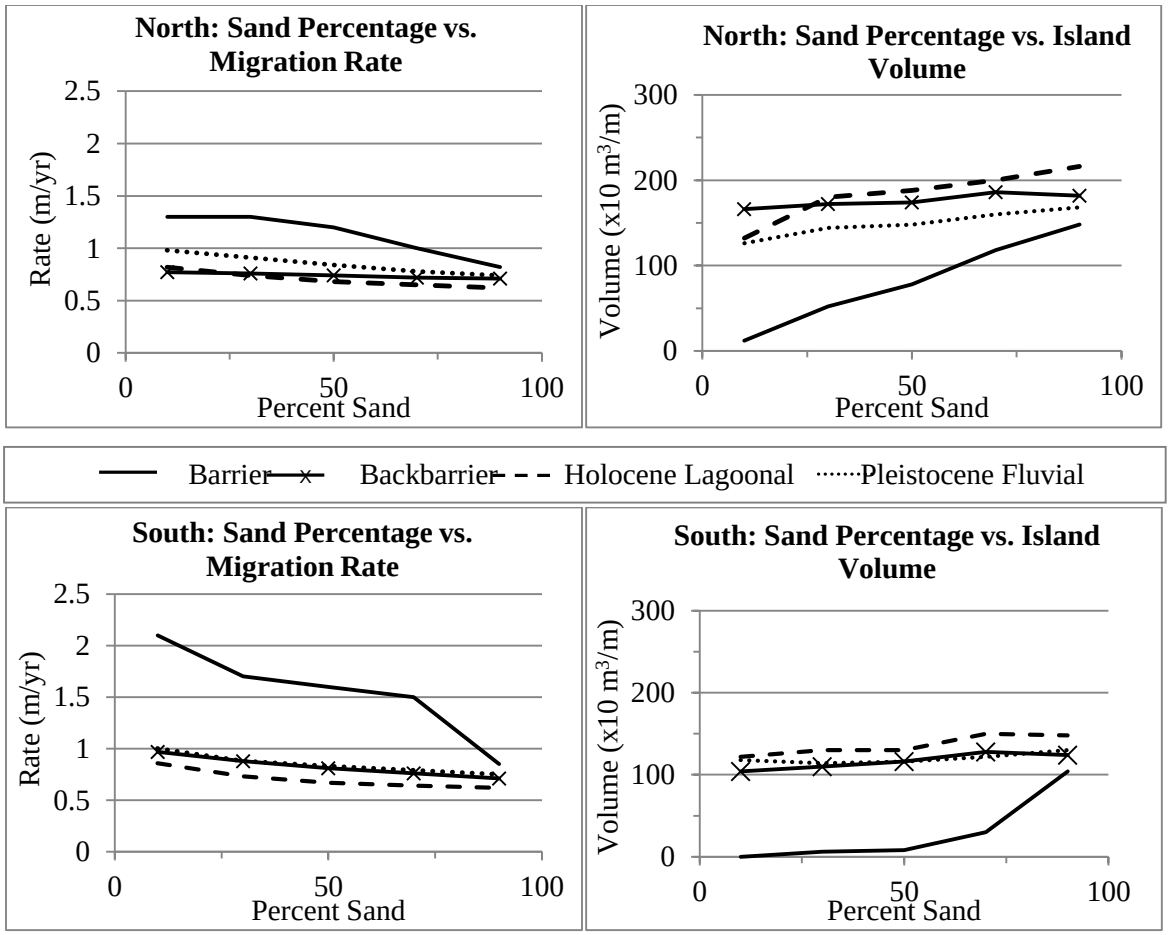
North: Sand Percentage vs. Migration Rate
Rate (m/yr)
2.5
2
1.5
1
0.5
0
0
50
100
Percent Sand
North: Sand Percentage vs. Island Volume
Volume (x10 m3/m)
300
200
100
0
0
50
100
Percent Sand
Barrier
Backbarrier
Holocene Lagoonal
Pleistocene Fluvial
South: Sand Percentage vs. Migration Rate
Rate (m/yr)
2.5
2
1.5
1
0.5
0
0
50
100
Percent Sand
South: Sand Percentage vs. Island Volume
Volume (x10 m3/m)
300
200
100
0
0
50
100
Percent Sand

Figure 10

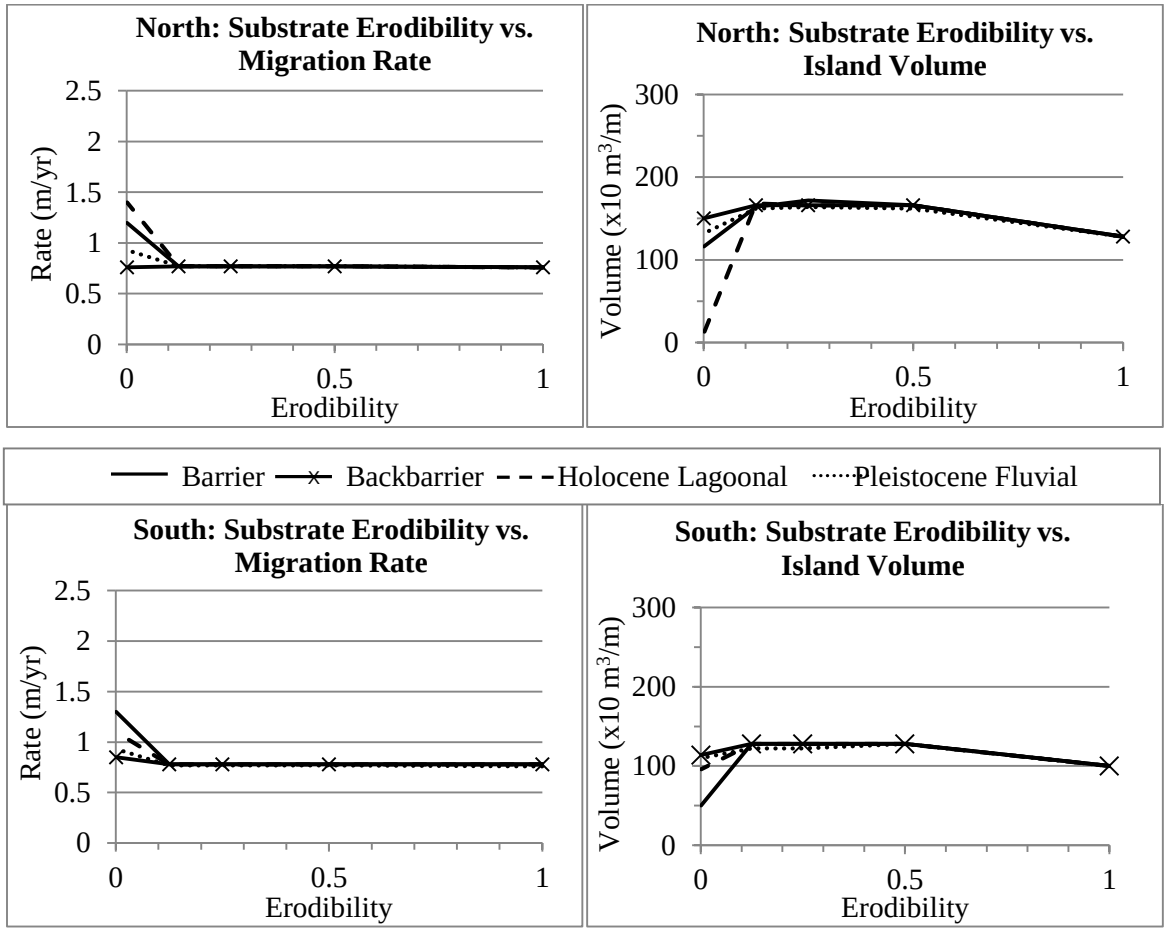
North: Substrate Erodibility vs. Migration Rate
Rate (m/yr)
2.5
2
1.5
1
0.5
0
0
0.5
1
Erodibility
North: Substrate Erodibility vs. Island Volume
Volume (x10 m3/m)
300
200
100
0
0
0.5
1
Erodibility
Barrier
Backbarrier
Holocene Lagoonal
Pleistocene Fluvial
South: Substrate Erodibility vs. Migration Rate
Rate (m/yr)
2.5
2
1.5
1
0.5
0
0
0.5
1
Erodibility
South: Substrate Erodibility vs. Island Volume
Volume (x10 m3/m)
300
200
100
0
0
0.5
1
Erodibility

Figure 11

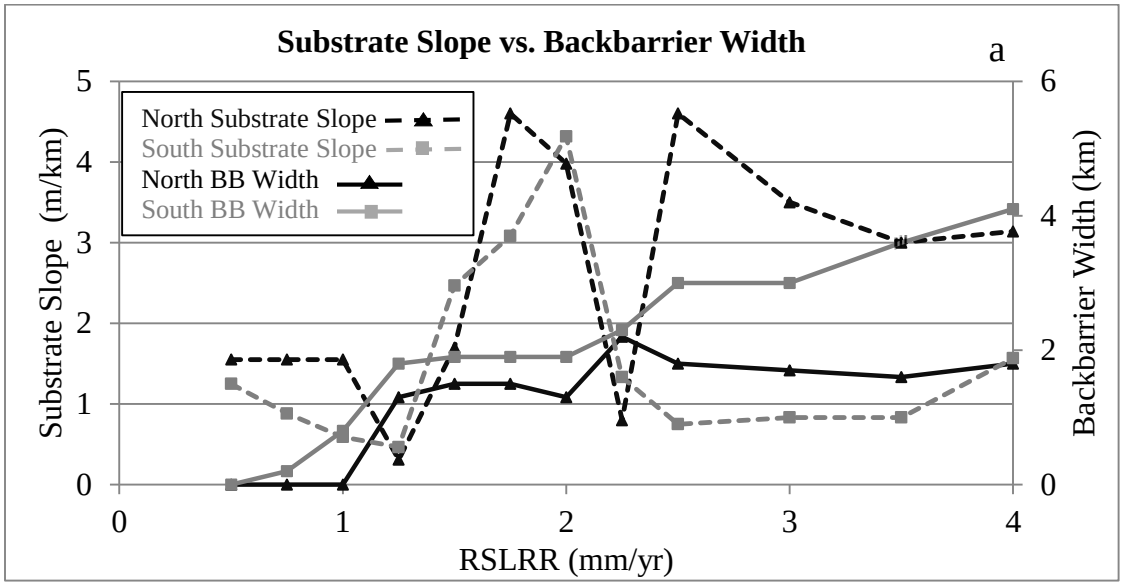
Substrate Slope vs. Backbarrier Width
a
North Substrate Slope
South Substrate Slope
North BB Width
South BB Width
Substrate Slope (m/km)
Backbarrier Width (km)
RSLRR (mm/yr)
0
1
2
3
4
5
6

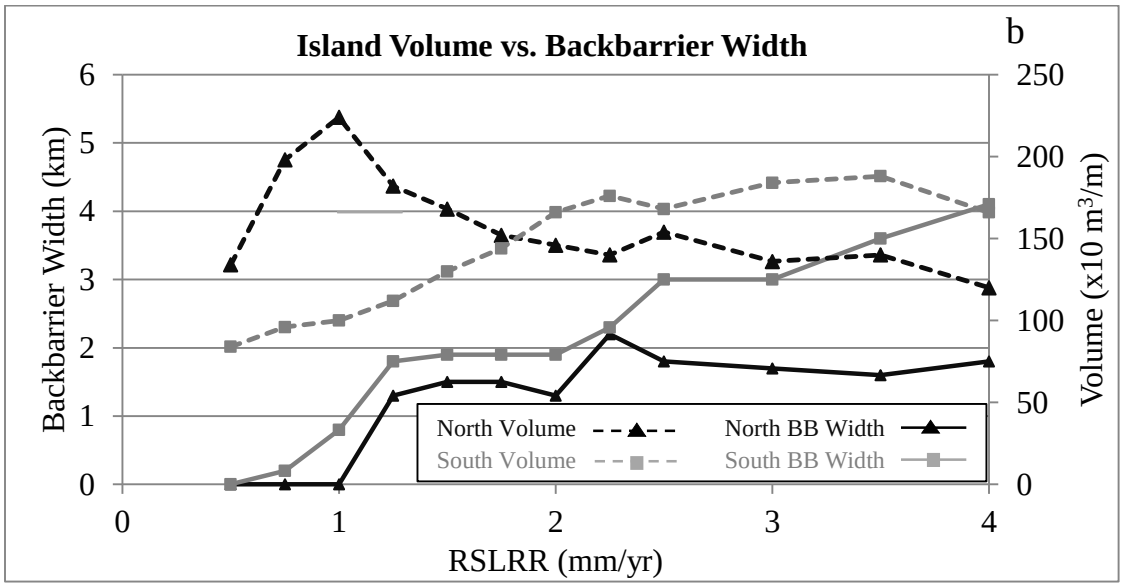
Island Volume vs. Backbarrier Width
b
North Volume
South Volume
North BB Width
South BB Width
Backbarrier Width (km)
Volume (x10 m3/m)
RSLRR (mm/yr)
0
50
100
150
200
250

Figure 12

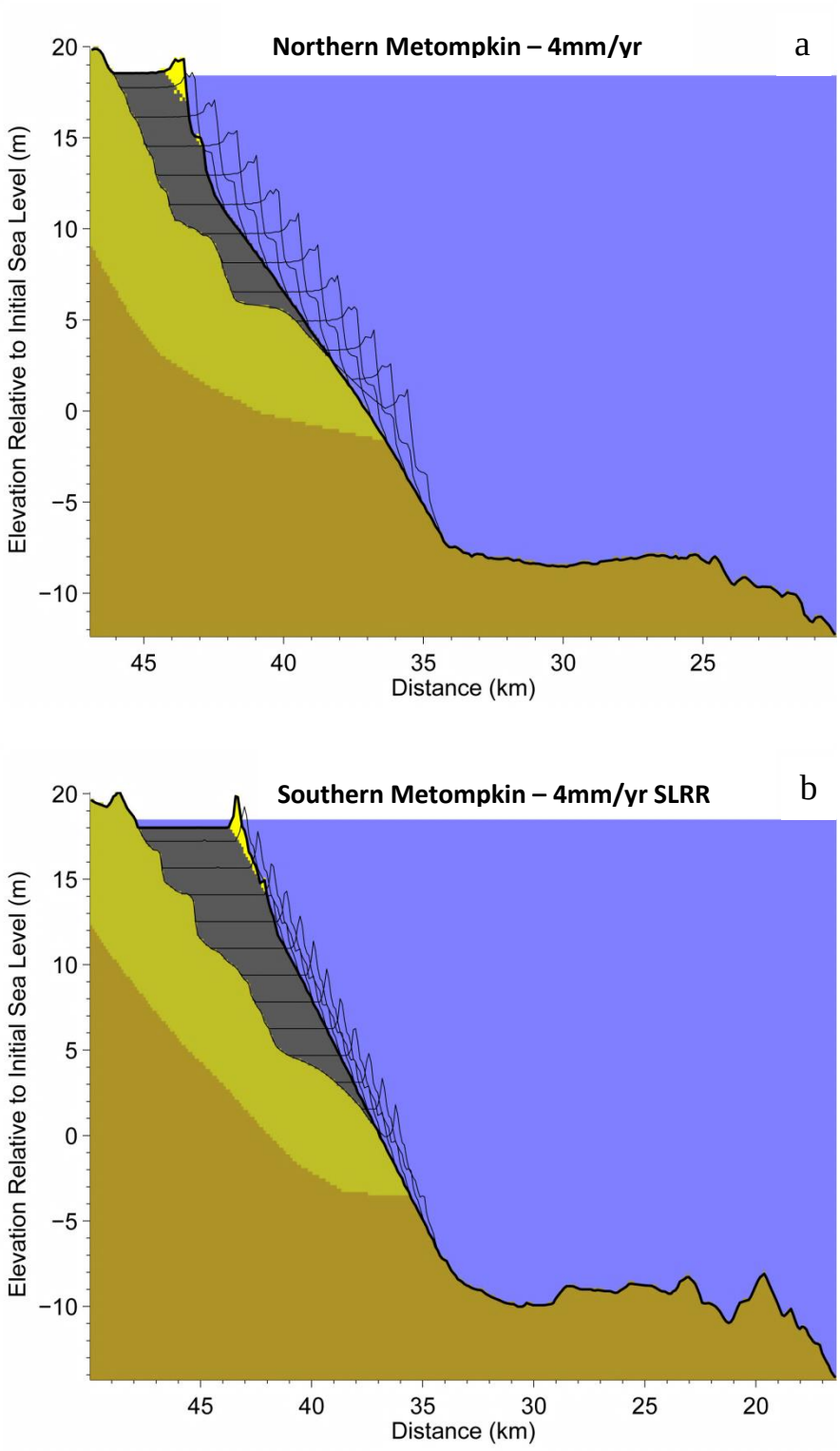
Northern Metompkin – 4mm/yr
a
Elevation Relative to Initial Sea Level (m)
20
15
10
5
0
−5
−10
45
40
35
30
25
Distance (km)
Southern Metompkin – 4mm/yr SLRR
b
Elevation Relative to Initial Sea Level (m)
20
15
10
5
0
−5
−10
45
40
35
30
25
20
Distance (km)

Figure 13

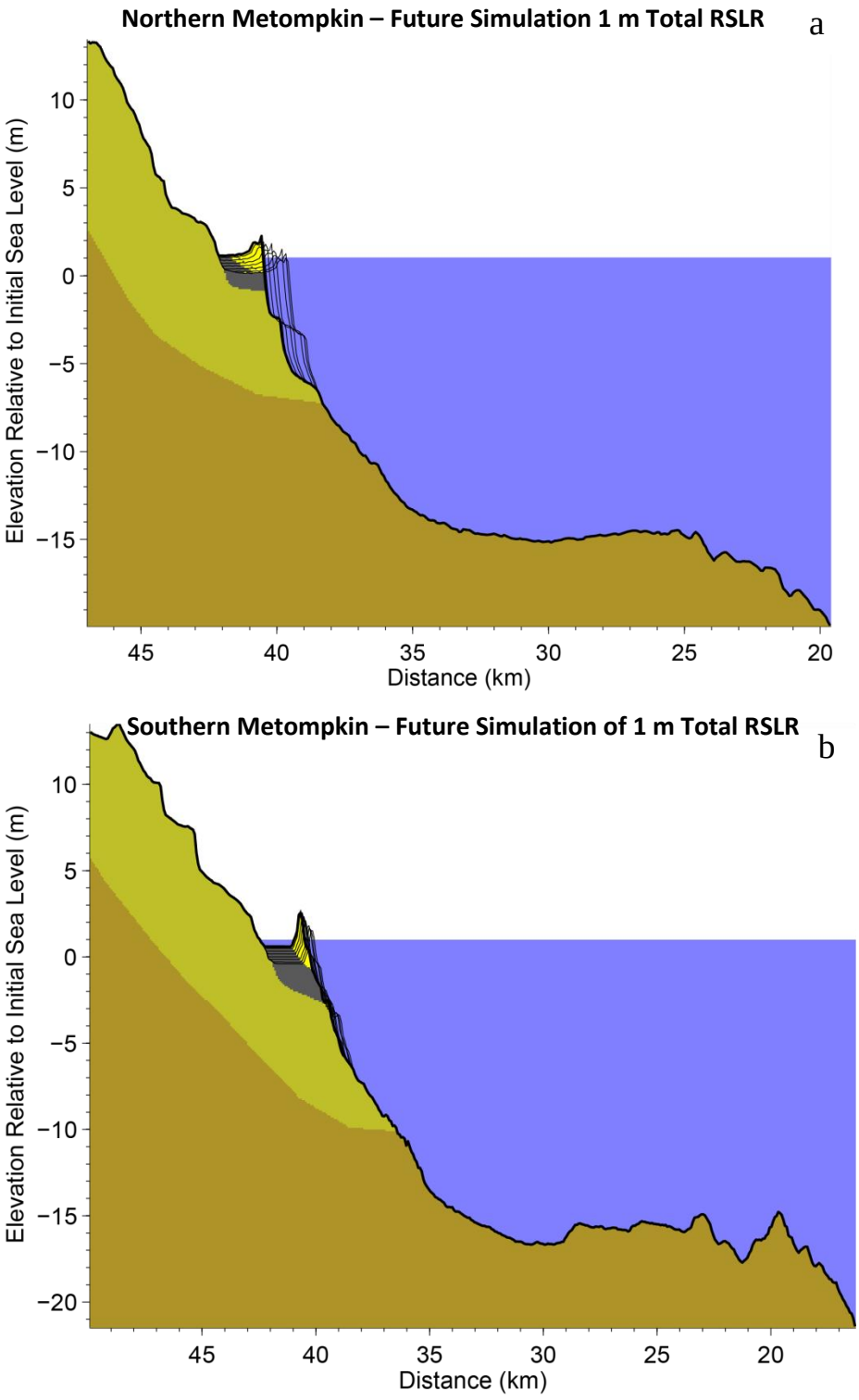
Northern Metompkin – Future Simulation 1 m Total RSLR
a
Elevation Relative to Initial Sea Level (m)
10
5
0
−5
−10
−15
45
40
35
30
25
20
Distance (km)
Southern Metompkin – Future Simulation of 1 m Total RSLR
b
Elevation Relative to Initial Sea Level (m)
10
5
0
−5
−10
−15
−20
45
40
35
30
25
20
Distance (km)

Figure 14

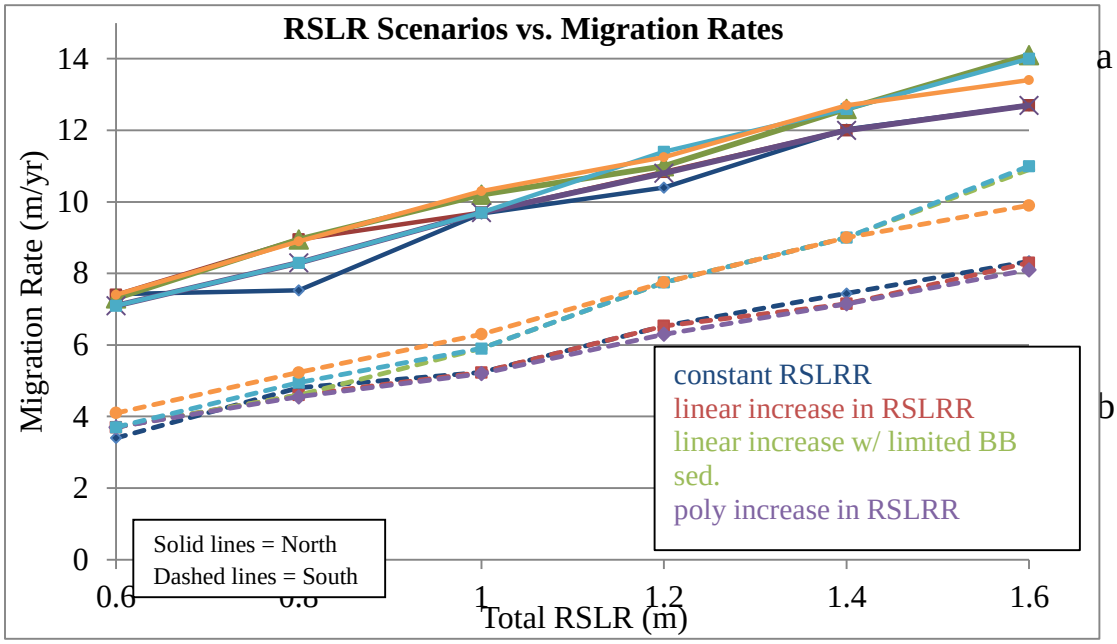
RSLR Scenarios vs. Migration Rates
Migration Rate (m/yr)
Total RSLR (m)
Solid lines = North
Dashed lines = South
constant RSLRR
linear increase in RSLRR
linear increase w/ limited BB sed.
poly increase in RSLRR
a
b

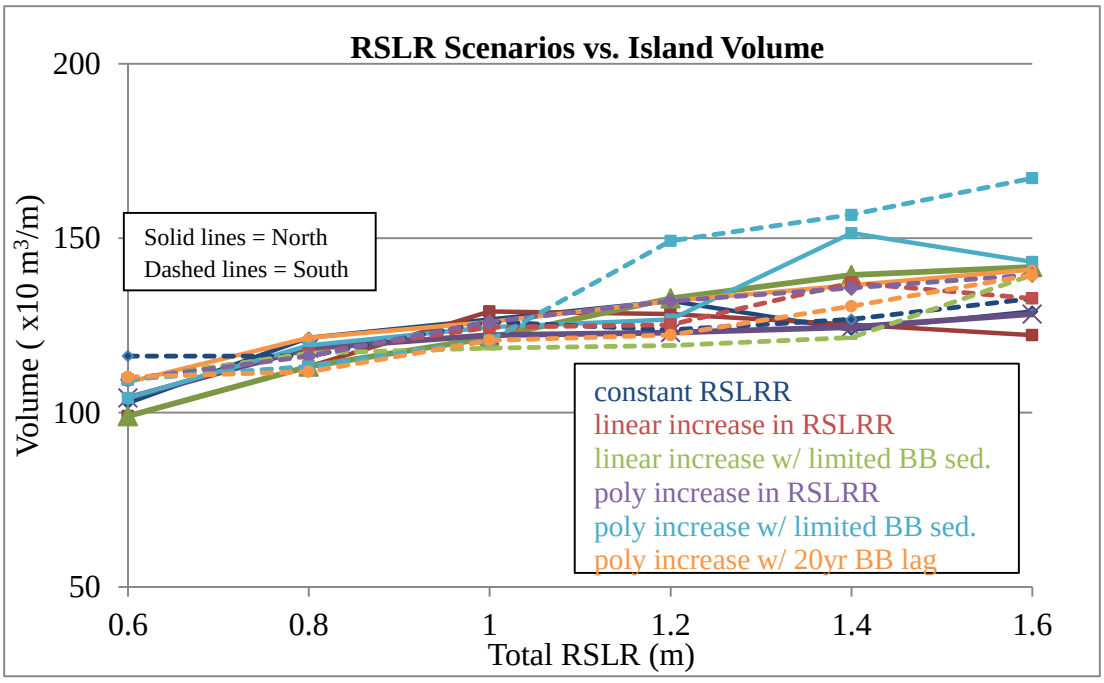
RSLR Scenarios vs. Island Volume
Volume ( x10 m3/m)
Total RSLR (m)
Solid lines = North
Dashed lines = South
constant RSLRR
linear increase in RSLRR
linear increase w/ limited BB sed.
poly increase in RSLRR
poly increase w/ limited BB sed.
poly increase w/ 20yr BB lag

Figure 15

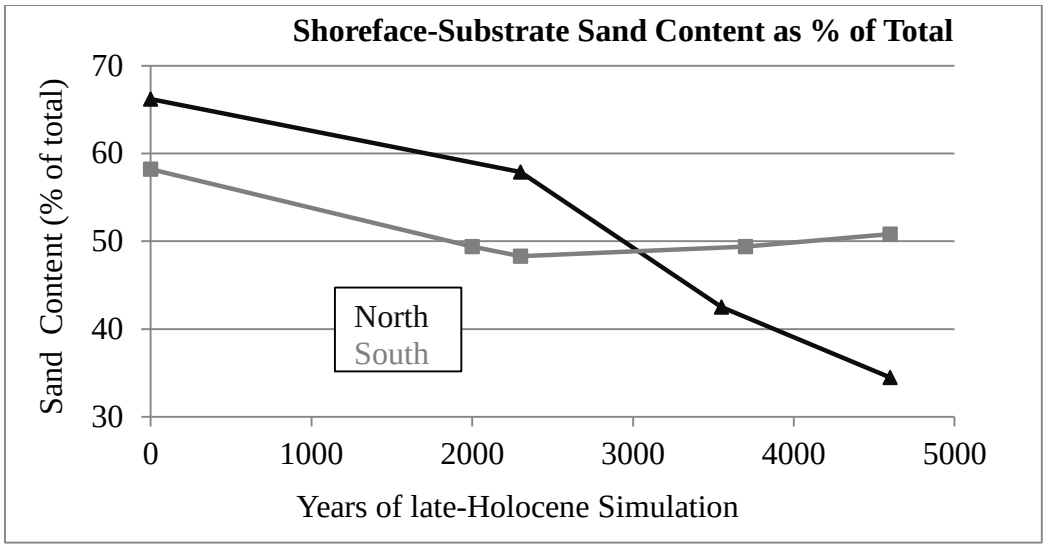
Shoreface-Substrate Sand Content as % of Total
Sand Content (% of total)
70
60
50
40
30
0
1000
2000
3000
4000
5000
Years of late-Holocene Simulation
North
South

Figure 16

1